<< Previous Chapter

Chapter 9

Eigenmatrix Methods

The inherent optical properties of natural water bodies usually depend on depth, and the solution methods developed in the previous chapters are able to solve the radiance transfer equation in water whose IOP's vary arbitrarily with depth. There would thus seem to be little justification for studying solution methods that are applicable only to homogeneous water bodies – those whose IOP's are independent of depth. However, the restriction to constant IOP's is not a serious one. We can always divide the water body into many thin layers, each with constant IOP's, but with different IOP's for different layers. A sufficiently fine division of this type can give an acceptable approximation to the actual depth profile of IOP's. We already have mentioned this approach in our discussion of Monte Carlo methods.

If a highly efficient solution method for homogeneous waters can be developed, then it may be advantageous overall to solve the RTE within each layer, and then to combine these "layer solutions" to obtain the solution of the RTE for an inhomogeneous water body. This is precisely the approach taken in the *discrete-ordinates* solution method, to be discussed in the next section.

We shall find that the discrete-ordinates approach leads to a matrix equation that has precisely the form of Eq. (8.57) for the spectral amplitudes. Now, however, the local transfer matrix $\underline{K}$ will be independent of depth. *The depth independence of $\underline{K}$ will allow us to solve the RTE as a matrix eigenvalue-eigenvector problem*, rather than resorting to the depth integration of differential equations. This matrix formulation also will enable us to establish a profound and useful connection with the fundamental-solution formalism of the previous two chapters. On the practical side, the eigenmatrix solution immediately gives the asymptotic radiance distribution $L_\infty(\mu)$ and asymptotic attenuation coefficient k_∞, which were introduced in Section 5.8. We also will learn how to compute the reflectance $\underline{\hat{r}}(m,\infty)$ of an infinitely deep, homogenous slab of water $S[m,\infty]$. Recall from Eq. (8.93) that $\underline{\hat{r}}(m,\infty)$ can be used in the specification of the bottom boundary condition for the integration of the Riccati equations.

In this chapter we shall make an additional assumption, namely that the water is free of any internal sources such as bioluminescence or light

inelastically scattered into the wavelength of interest. This is not a necessary assumption for our development. The discrete-ordinates method easily accommodates internal source terms, and they are routinely included in applications of the method to atmospheric radiative transfer problems. In the previous chapter we laboriously included the source terms in all equations, in order to show explicitly how they are handled. Now, however, we wish to concentrate on those aspects of the theory that are peculiar to homogeneous water bodies. Carrying along an internal source term in all equations would add little to our discussion; omitting the source terms will simplify the equations.

9.1 The Discrete-Ordinates Method

This powerful solution method is based on *approximating the scattering phase function as a series of Legendre polynomials, truncated to a finite number 2n of terms:*

$$\tilde{\beta}(\psi) \approx \sum_{k=0}^{2n-1} g_k P_k(\cos\psi) . \tag{9.1}$$

Here the g_k are the *expansion coefficients*, and the P_k are *Legendre polynomials*. It will prove convenient [see Eqs. (9.6) and (9.11)] to have an even number of terms in Eq. (9.1), hence the upper limit of $2n-1$ in the sum. For the moment, we consider n to be an arbitrary integer; we shall discuss below how to determine its value.

Legendre polynomials are treated in textbooks on mathematical methods of physics, for example Boas (1983) or Mathews and Walker (1965). They can be defined in general by

$$P_k(x) \equiv \frac{1}{2^k k!} \frac{d^k}{dx^k} (x^2 - 1)^k,$$

where $x = \cos\psi$ in the context of Eq. (9.1). The first few Legendre polynomials are

$$\begin{aligned} P_0(x) &= 1 & P_3(x) &= \frac{1}{2}(5x^3 - 3x) \\ P_1(x) &= x & P_4(x) &= \frac{1}{8}(35x^4 - 30x^2 + 3) \\ P_2(x) &= \frac{1}{2}(3x^2 - 1) & P_5(x) &= \frac{1}{8}(63x^5 - 70x^3 + 15x). \end{aligned} \tag{9.2}$$

The P_k form a complete set of orthogonal functions on the interval $-1 \le x \le 1$. They satisfy the orthogonality relation

$$\int_{-1}^{1} P_k(x)\, P_m(x)\, dx \;=\; \frac{2}{2m+1}\,\delta_{k,m}\,, \tag{9.3}$$

where $\delta_{k,m}$ is the Kronecker delta function of Eq. (1.19).

Multiplying Eq. (9.1) by $P_m(\cos\psi)\sin\psi$, integrating over ψ, and using Eq. (9.3) gives the expansion coefficients:

$$\begin{aligned} g_m \;&=\; \frac{2m+1}{2} \int_0^{\pi} \tilde{\beta}(\psi)\, P_m(\cos\psi)\, \sin\psi\, d\psi \\ &=\; \frac{2m+1}{2} \int_{-1}^{1} \tilde{\beta}(x)\, P_m(x)\, dx\,. \end{aligned} \tag{9.4}$$

Chandrasekhar (1960) shows that if $\tilde{\beta}(\psi)$ is written as $\tilde{\beta}(\mu',\phi'\to\mu,\phi)$, then the expression equivalent to Eq. (9.1) is

$$\tilde{\beta}(\mu',\phi'\to\mu,\phi) \;= \sum_{l=0}^{2n-1} (2-\delta_{0,l}) \left[\sum_{k=l}^{2n-1} g_k^{\,l}\, P_k^{l}(\mu)\, P_k^{l}(\mu') \right] \cos l(\phi-\phi')\,, \tag{9.5}$$

where

$$g_k^{\,l} \;\equiv\; g_k\, \frac{(k-l)!}{(k+l)!}\,,$$

and the $P_k^{\,l}$ are *associated Legendre polynomials*, defined by

$$P_k^{l}(x) \;\equiv\; (1-x^2)^{l/2}\, \frac{d^{\,l}}{dx^{\,l}}\, P_k(x)\,,$$

for $l = 0, 1, ..., 2n-1$ and $k = l, ..., 2n-1$. Note that in $g_k^{\,l}$ and $P_k^{\,l}$, the superscript l denotes an index, not the l^{th} power.

The reason for choosing Legendre polynomials as the basis for expansion of the phase function is that they are mathematically consistent with an expansion of the radiance as a Fourier cosine series (Shifrin, *et al.*, 1972):

$$L(\zeta;\mu,\phi) \;\approx\; \sum_{l=0}^{2n-1} \hat{L}(\zeta;\mu;l)\cos l(\phi-\phi_o)\,. \tag{9.6}$$

Just as in Chapter 8, $\hat{L}$ denotes a Fourier radiance amplitude. Now,

however, we are dealing with a *continuous function of* μ *and* ϕ – no mention has been made of quad averaging. Consequently, the value of n is still unspecified, and the radiance amplitudes are given by

$$\hat{L}(\zeta;\mu;l) = \frac{1}{\pi(1+\delta_{0,l})}\int_0^{2\pi} L(\zeta;\mu,\phi)\cos(l\phi)\,d\phi\,,$$

which is the continuous-function equivalent of Eq. (8.22). Note also that the presence of the arbitrary phase angle ϕ_o in Eq. (9.6) makes this equation equivalent to an expansion of L in sines and cosines, as was done (for the discrete case) in Eq. (8.31).

Because of the mathematical consistency between Fourier expansions of L and Legendre expansions of $\tilde{\beta}$, the exact infinite-series versions (i.e, replace $2n-1$ by ∞) of Eqs. (9.1), (9.5) and (9.6) are often used in theoretical radiative transfer studies, even when the discrete-ordinates method is not being employed. Many such examples can be found in the papers collected by Kattawar (1991).

Reduction of the RTE to matrix form

The RTE (5.24), written for the special case of depth-independent IOP's and source-free water, is

$$\mu\frac{dL(\zeta;\mu,\phi)}{d\zeta} = -L(\zeta;\mu,\phi) + \omega_o\int_0^{2\pi}\int_{-1}^{1} L(\zeta;\mu',\phi')\,\tilde{\beta}(\mu',\phi'\to\mu,\phi)'\,d\mu'\,d\phi'\,. \tag{9.7}$$

The next step in the development of the discrete-ordinates method is to substitute Eqs. (9.5) and (9.6) into Eq. (9.7). The rather messy result is then simplified by noting that

$$\int_0^{2\pi}\cos l(\phi'-\phi_o)\cos m(\phi-\phi')\,d\phi' = \pi(\delta_{l,m}+\delta_{l,-m})\cos l(\phi-\phi_o)\,.$$

All terms in the resulting equations involve $\cos l(\phi-\phi_o)$. Recalling the linear independence of $\cos l(\phi-\phi_o)$ for different l values [just as in the development of Eqs. (8.37) and (8.38)] decouples the spectral from Eq. (9.7) into $2n$ independent equations of the form

$$\mu \frac{d\hat{L}(\zeta;\mu;l)}{d\zeta} = -\hat{L}(\zeta;\mu;l) + 2\pi\omega_o \sum_{k=l}^{2n-1} g_k^l P_k^l(\mu) \int_{-1}^{1} \hat{L}(\zeta;\mu';l) P_k^l(\mu') d\mu' . \tag{9.8}$$

where $l = 0, 1, ..., 2n-1$.

We next approximate the integral in Eq. 9.8) as a summation. This is usually done by double Gauss-Legendre quadrature, in which an integral over $-1 \le \mu \le 1$ is written as

$$\begin{aligned} \int_{-1}^{1} f(\mu)\, d\mu &= \int_{-1}^{0} f(\mu)\, d\mu + \int_{0}^{1} f(\mu)\, d\mu \\ &= \sum_{j=-n}^{-1} a_j f(\mu_j) + \sum_{j=1}^{n} a_j f(\mu_j) \\ &= \sum_{j=1}^{n} a_{-j} f(\mu_{-j}) + \sum_{j=1}^{n} a_j f(\mu_j). \end{aligned} \tag{9.9}$$

Here the a_j's are weights corresponding to the abscissa points μ_j. Both the a_j's and μ_j's are determined in a straightforward manner from the roots of the Legendre polynomial $P_{2n}(\mu)$. The details of these computations need not concern us here; we note only that $a_{-j} = a_j$ and $\mu_{-j} = -\mu_j$. The rationale for this quadrature scheme is discussed, for example, in Stamnes, *et al.* (1988). Algorithms and computer code for computing the a_j's and μ_j's are found in Press, *et al.* (1986).

Applying Eq. (9.9) to (9.8) gives

$$\begin{aligned} \mu_i \frac{d\hat{L}(\zeta;\mu_i;l)}{d\zeta} &= -\hat{L}(\zeta;\mu_i;l) \\ &\quad + 2\pi\omega_o \sum_{k=l}^{2n-1} g_k^l P_k^l(\mu_i) \\ &\quad \times \left[\sum_{j=1}^{n} a_{-j} \hat{L}(\zeta;\mu_{-j};l) P_k^l(\mu_{-j}) + \sum_{j=1}^{n} a_j \hat{L}(\zeta;\mu_j;l) P_k^l(\mu_j) \right], \end{aligned} \tag{9.10}$$

or

$$\mu_i \frac{d\hat{L}_i(\zeta;l)}{d\zeta} = -\hat{L}_i(\zeta;l) + \sum_{j=1}^{n} \hat{L}_{-j}(\zeta;l)\, C_{-j,i} + \sum_{j=1}^{n} \hat{L}_j(\zeta;l)\, C_{j,i} . \tag{9.11}$$

Note that in going from Eq. (9.8) to (9.10) via (9.9), we have replaced the continuous μ variable by the discrete values μ_i, $i = -n, ..., -1, 1, ..., n$,

determined as in Eq. (9.9). *This is the manner in which the discrete-ordinates method discretizes the polar angle* μ.

In going from Eq. (9.10) to (9.11) we have merely rearranged terms and defined

$$\hat{L}_i(\zeta;l) \equiv \hat{L}(\zeta;\mu_i;l) \tag{9.12}$$

and

$$C_{j,i}(l) \equiv 2\pi\omega_o \sum_{k=l}^{2n-1} a_j g_k^l P_k^l(\mu_i) P_k^l(\mu_j) \tag{9.13}$$

for $i, j = -n, ..., -1, 1, ..., n$.

It should be noted that *the* $C_{j,i}$ *are known quantities that depend only on the IOP's* (both directly via ω_o and indirectly via the expansion coefficients of $\tilde{\beta}$) *and on the quadrature weights.*

Definitions (9.12) and (9.13) are made in order to highlight the matrix character of the amplitude Eq. (9.11). Note that Eq. (9.11) splits into two sets of equations. The set with $i < 0$ corresponds to upwelling radiances ($\mu_i < 0$, or $\mu_i \in \Xi_u$); the set with $i > 0$ corresponds to downwelling radiances ($\mu_i > 0$, or $\mu_i \in \Xi_d$). Recall that $\mu_{-i} = -\mu_i$. It is therefore convenient to define two $1\times n$ matrices.

$$\underline{\hat{L}}^-(\zeta;l) \equiv \left[\hat{L}_{-1}(\zeta;l), ..., \hat{L}_{-n}(\zeta;l)\right]$$

and (9.14)

$$\underline{\hat{L}}^+(\zeta;l) \equiv \left[\hat{L}_1(\zeta;l), ..., \hat{L}_n(\zeta;l)\right].$$

Finally, we define $n\times n$ matrices $\underline{\hat{\mathfrak{t}}}$ and $\underline{\hat{\rho}}$ via

$$[\underline{\hat{\mathfrak{t}}}]_{ji} \equiv \frac{1}{\mu_i}(C_{j,i} - \delta_{j,i}) = \frac{1}{\mu_i}(C_{-j,-i} - \delta_{j,i}) \tag{9.15}$$

and

$$[\underline{\hat{\rho}}]_{ji} \equiv \frac{1}{\mu_i} C_{-j,i} = \frac{1}{\mu_i} C_{j,-i}. \tag{9.16}$$

Equation (9.11) can then be written as a matrix equation

$$\frac{d}{d\zeta}[\underline{\hat{L}}^-(\zeta;l), \underline{\hat{L}}^+(\zeta;l)] = [\underline{\hat{L}}^-(\zeta;l), \underline{\hat{L}}^+(\zeta;l)] \begin{bmatrix} -\underline{\hat{\mathfrak{t}}}(l) & \underline{\hat{\rho}}(l) \\ -\underline{\hat{\rho}}(l) & \underline{\hat{\mathfrak{t}}}(l) \end{bmatrix}. \tag{9.17}$$

Proceeding one step further, we define the $1\times 2n$ matrix

$$\underline{\hat{L}}(\zeta;l) \equiv [\underline{\hat{L}}^{-}(\zeta;l), \underline{\hat{L}}^{+}(\zeta;l)] , \tag{9.18}$$

and the $2n \times 2n$ matrix

$$\underline{K}(l) \equiv \begin{bmatrix} -\underline{\hat{\tau}}(l) & \underline{\hat{\rho}}(l) \\ -\underline{\hat{\rho}}(l) & \underline{\hat{\tau}}(l) \end{bmatrix} . \tag{9.19}$$

Then Eq. (9.17) becomes just

$$\frac{d}{d\zeta} \underline{\hat{L}}(\zeta;l) = \underline{\hat{L}}(\zeta;l) \underline{K}(l) , \tag{9.20}$$

where $l = 0, 1, ..., 2n-1$.

We hope that the reader now has a strong feeling of *d j vu. Equation (9.20) has precisely the same mathematical form as the matrix Eq. (8.59) of the previous chapter, when Eq. (8.59) is written for the case of source-free water and depth-independent IOP's.* The last few equations should be compared with their counterparts in Chapter 8. Now $\underline{K}(l)$ is a $2n \times 2n$ matrix (with n still unspecified) whose elements depend only on the constant IOP's and on the details of discretization of the angular variables (i.e., on the weights a_j and on the expansion coefficients g_l). In Chapter 8, $\underline{K}(l)$ was $2m \times 2$m and depended only on the IOP's and on the details of discretization (i.e., on the choice of a quad-averaging scheme, which fixed the value of m). The similarities and differences in the $\underline{\hat{\tau}}$ and $\underline{\hat{\rho}}$ matrices can be seen by comparing Eqs. (9.15) and (9.16) with Eqs. (8.42), and so on.

Both quad averaging and the steps so far described in the development of the discrete-ordinates method are just two different ways of discretizing the direction variables in the RTE. Both methods start from the same equation and will presumably arrive at the same answer, so it should come as no surprise that some of the intermediate equations bear a strong resemblance to each other[1]. Much of the remainder of this chapter will

---

[1]Be forewarned that discrete-ordinates literature often applies the method to atmospheric problems with ζ positive upward, which reverses the directional meaning of the + and − labels seen in Eq. (9.18). Also, Eq. (9.20) is usually seen in its transpose form $d\underline{\hat{L}}/d\zeta = \underline{K}\,\underline{\hat{L}}$, where $\underline{\hat{L}}$ is a $2n \times 1$ array and $\underline{K}$ has the form

discuss the solutions of equations of the *form* of Eq. (9.20). We need not worry about whether the elements of $\underline{K}(l)$ came from quad averaging, from discrete ordinates, or from some other discretization scheme. Before proceeding with that discussion, however, we must answer the question of how to choose the value of n in Eq. (9.1).

Choosing the number of terms in the phase function expansion

Equation (9.1) gives an exact representation of any $\tilde{\beta}$ if the right hand side is an infinite series. In practice, we must pick a finite value of n that is large enough that the right hand side of Eq. (9.1) is acceptably close to the value of the actual phase function $\tilde{\beta}(\psi)$ at all scattering angles $0 \le \psi \le \pi$. The choice of n is often made by numerical trial of error and, of course, "acceptably close" depends on the accuracy needed in the solution of the problem at hand.

For phase functions that are *not* highly peaked, relatively few terms are necessary. For example, Kattawar (1975) shows that the Henyey-Greenstein phase function $\tilde{\beta}_{\text{HG}}$ of Eq. (3.34) has the expansion coefficients

$$g_k = \frac{2k+1}{4\pi} g^k, \tag{9.21}$$

where g is the asymmetry parameter (the average of $\cos\psi$) defined in general in Eq. (3.8b) and evaluated for $\tilde{\beta}_{\text{HG}}$ in Eq. (3.35). Since the Henyey-Greenstein g_k's depend on powers of g, the values of g_k decrease quickly with increasing k for values of g less than roughly 0.8. This is the case for, say, the atmospheric-haze phase function seen in Fig. 3.14, which has $g = 0.66$ [or $g_1 = 0.71$ and $g_2 = -0.76$ when fit with a TTHG phase function as in Eq. (3.36)].

However, if the phase function is highly peaked, like $\tilde{\beta}_{\text{p}}$ or $\tilde{\beta}_{\text{cirrus}}$ in Fig. 3.14, then many hundreds of terms may be required in Eq. (9.1) in order to achieve a satisfactory expansion of $\tilde{\beta}$. This slow convergence is illustrated in Fig. 9.1 for the particle phase function $\tilde{\beta}_{\text{p}}$ of Table 3.10. The

---

$$\begin{bmatrix} -\hat{\underline{\tau}}^{\text{T}} & -\hat{\underline{\rho}}^{\text{T}} \\ \hat{\underline{\rho}}^{\text{T}} & \hat{\underline{\tau}}^{\text{T}} \end{bmatrix},$$

where "T" denote the matrix transpose. The right hand side of Eq. (9.13) then corresponds to $C_{i,j}$, rather than to $C_{j,i}$. We have chosen the present form of Eq. (9.20) for consistency with Eq. (8.58).

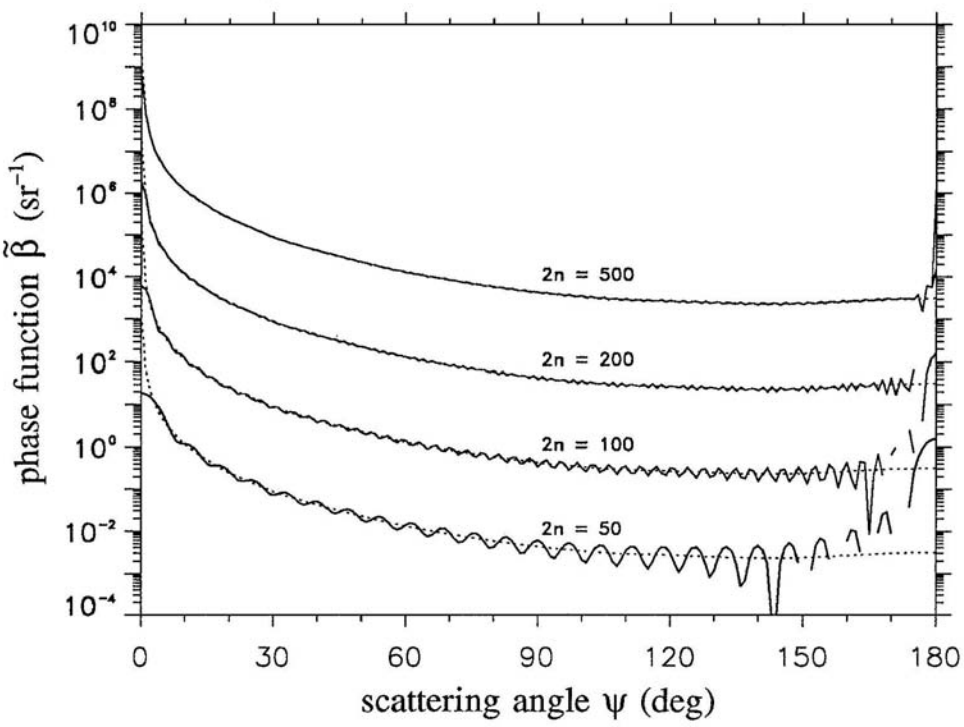

Fig. 9.1. Expansion of the particle phase function $\tilde{\beta}_p$ of Table 3.10 in a series of Legendre polynomials according to Eq. (9.1). The dotted lines give $\tilde{\beta}_p$, and the solid lines give the right hand side of Eq. (9.1) for different numbers $2n$ of terms in the sum. The ordinate axis refers to the curve for $2n = 50$; subsequent curves are displaced by factors of 100 for clarity. Gaps in the solid lines are regions where the sum is negative.

figure shows the right hand side of Eq. (9.1) for $2n$ = 50, 100, 200 and 500 total terms in the sum. Gaps in the plotted curves are regions where the sum is *negative*; such poor approximations to $\tilde{\beta}$ are unacceptable on physical grounds. The expansion coefficients were computed by (double precision) numerical integration of Eq. (9.4). Even when 500 terms are included in the $\tilde{\beta}_p$ expansion, the sum still differs noticeably from $\tilde{\beta}_p(\psi)$ at very small and very large ψ. The convergence of the series (9.1) is very slow when $x \equiv \cos\psi \approx 1$ because of the highly peaked behavior of $\tilde{\beta}_p$ as $x \to 1$. The convergence is slow when $x \approx -1$ (i.e. when $\psi \approx 180°$) because the Legendre polynomials alternate in sign, as can be seen by setting $x = -1$ in Eq. (9.2).

If we must include hundreds of terms in (9.1), then the matrices in Eq. (9.20) become too large for efficient computation and, moreover, hundreds of such equations must be solved (one for each l value). The discrete-ordinates method then becomes computationally impracticable.

Various tricks are used to circumvent the problems inherent in Eq. (9.1). A common procedure is to regard radiance scattered by only a few degrees as being unscattered, in which case the actual phase function $\tilde{\beta}(\psi)$ can be approximated as a Dirac delta function plus a less-peaked or "smoother" phase function that describes large-angle scattering. For example, *the Delta-M approximation* of Wiscombe (1977) writes

$$\tilde{\beta}(\psi) \approx 2f\,\delta(1-\cos\psi) + (1-f)\,\tilde{\beta}^*(\psi)\,, \tag{9.22a}$$

or equivalently

$$\tilde{\beta}(\mu',\phi'\rightarrow\mu,\phi) \approx 2f\,\delta(\mu-\mu')\,\delta(\phi-\phi') + (1-f)\,\tilde{\beta}^*(\mu',\phi'\rightarrow\mu,\phi)\,, \tag{9.22b}$$

where f is the fraction ($0 \le f \le 1$) of "unscattered" radiance, δ is the Dirac delta function of Eq. (1.15), and $\tilde{\beta}^*$ is a "smooth" phase function that describes the scattered radiance. The factor of 2 in the δ-function term occurs because δ is being used at the endpoint of an integration interval; it is a property of δ that

$$\int_{-1}^{1} \delta(1-\cos\psi)\,d\cos\psi = \frac{1}{2}\,.$$

If $\tilde{\beta}$, $\tilde{\beta}^*$, and δ are each expanded in Legendre polynomials, then f and the expansion coefficients g_k^* of $\tilde{\beta}^*$ can be determined from the expansion coefficients g_k of $\tilde{\beta}$ in such a manner that $\tilde{\beta}$ and the right hand side of Eq. (9.22) agree for the first $2M$ terms of their Legendre polynomial expansions. The radiative transfer effects of small-angle scattering are then accounted for by analytical treatment of the δ-function in the RTE (see problem 9.3), and the large-angle scattering described by $\tilde{\beta}^*$ receives a numerical treatment. The resulting numerical equations corresponding to Eqs. (9.11) or (9.20) are then of order M in size, not of order n, where $M << n$.

Approximations like Eq. (9.22) can yield very accurate computations of *irradiance* for small M. However, if the details of the forward-scattered radiance distribution are important, then approximations like Eq. (9.22) are inadequate and the exact $\tilde{\beta}$ must be used.

Completing the solution

The mathematical form of Eq. (9.20) suggests that $\hat{\underline{L}}$ behaves like an exponential function of ζ. Therefore, the next step of the discrete-ordinates method is to *seek solutions of Eq. (9.20) that have the form*

$$\hat{\underline{L}}(\zeta;l) = \underline{G}(l) \exp[-\kappa(l)\,\zeta]\,, \tag{9.23}$$

where $\underline{G}(l)$ is a $1\times 2n$ matrix for each l value. Substituting Eq. (9.23) into Eq. (9.20) gives a standard eigenvalue-eigenvector equation.

$$-\kappa(l)\,\underline{G}(l) = \underline{G}(l)\,\underline{\boldsymbol{K}}(l)\,. \tag{9.24}$$

Because the matrix $\underline{\boldsymbol{K}}$ is independent of depth, so are its eigenvalues κ and eigenvectors $\underline{G}$. Moreover, since $\underline{\boldsymbol{K}}$ is $2n\times 2n$, there are $2n$ linearly independent eigenvalues and eigenvectors, which we label κ_j and $\underline{G}_j$, $j = 1, 2, \ldots, 2n$. (Because of the structure of $\underline{\boldsymbol{K}}$, degenerate eigenvalues do not occur; see Section 9.4.) The general solution of Eq. (9.20) is a linear combination of these eigenvectors:

$$\hat{\underline{L}}(\zeta;l) = \sum_{j=1}^{2n} A_j(l)\,\underline{G}_j(l) \exp[-\kappa_j(l)\,\zeta]\,. \tag{9.25}$$

Here the A_j are arbitrary constants, which are to be determined by the boundary conditions imposed in the particular problem at hand. Note that although Eq. (9.23) is an exponential, the general solution (9.25) shows that $\hat{\underline{L}}(\zeta;l)$ is *not* an exponential: *it is a sum of exponentials that decay with depth at different rates.*

We shall not pursue the determination of the A_j, since we have now seen the essence of the discrete-ordinates method and, just as importantly, we have made a connection with the matrix equations of Chapter 8. This connection will allow us to investigate Eq. (9.25) from a slightly different viewpoint, starting in the next section.

Details of the remaining discrete ordinates calculations can be found, for example, in Stamnes, *et al.* (1988). That paper also shows how to include internal source terms. Methods for handling layered media are described in Jin and Stamnes (1993). Other important papers on discrete ordinates are found in Kattawar (1991). The basic concepts of the method originated with Wick (1943) and Chandrasekhar (1960). The mathematical nature of Eq. (9.25) as n becomes infinite can be treated with the singular

eigenfunction method, which is discussed, for example, in Case (1960), Case and Zweifel (1967), and Ku čer and McCormick (1991).

Strengths and weaknesses

We can now summarize the strengths and weaknesses of the discrete-ordinates method.

- It is a *very efficient way to compute irradiances.* Irradiances are computed from azimuthally integrated radiances, which correspond to the $l = 0$ case of Eqs. (9.6) or (9.20). Thus, solutions need be computed only for $l = 0$ in order to compute irradiances.

- *Radiance distributions are easily computed at any depth in homogeneous water.* Because of the simple analytic depth dependence of $\hat{\underline{L}}(\zeta;l)$ seen in Eq. (9.25), radiances are available at any depth ζ once the eigenvalue-eigenvector problem has been solved. Thus the computational costs are independent of the water depth.

- *Radiances are computed in specific directions*. This is in contrast to the directionally (quad) averaged radiance computed in Chapter 8. Discrete ordinates is an "*n-stream*" solution method, in the sense mentioned in Section 5.10.

- The method becomes numerically *inefficient if detailed radiance distributions are required for highly peaked phase functions*. In this case, it may be impossible to circumvent the "large n" requirements of the Legendre polynomial representation of $\tilde{\beta}$.

- The method becomes *inefficient if the IOP's are depth dependent*. If many homogeneous layers are required in order to approximate the depth behavior of the IOP's, then many eigenmatrix solutions are required. In addition, the individual layer solutions must be coupled together in order to determine the A_j's of each layer.

- It is *difficult to include the effects of wind-blown air-water surfaces*. This can be done in principle, but no computer codes incorporating random sea surfaces have been published.

9.2 A General Matrix Formulation of the Local Interaction Principles

In the previous section we encountered a matrix equation of the form

$$\frac{d}{d\zeta}\,\underline{\hat{L}}(\zeta) \;=\; \underline{\hat{L}}(\zeta)\,\underline{K}\,, \tag{9.26}$$

where we have dropped the l argument for brevity. Chapter 8 also produces such an equation in the case of source-free, homogeneous water. We also recall from Eq. (8.61) that the fundamental solution $\underline{\mathbf{M}}$ satisfies such an equation. The mapping property of the fundamental solution gives the radiance amplitudes at depth ζ from the amplitudes at some other depth, say w:

$$\underline{\hat{L}}(\zeta) \;=\; \underline{\hat{L}}(w)\,\underline{\mathbf{M}}(w,\zeta)\,. \tag{9.27}$$

[Recall Eq. (8.63) for source-free water.]

In the discrete-ordinates method, we obtained a solution of Eq. (9.26) by *assuming* that $\underline{\hat{L}}(\zeta)$ had an exponential form;

$$\underline{\hat{L}}(\zeta) \;=\; \underline{G}\exp[-\kappa\zeta]\,. \tag{9.28}$$

This assumption led to an eigenvalue-eigenvector equation for κ and $\underline{G}$. Comparing Eqs. (9.27) and (9.28) and noting that both $\underline{\hat{L}}$ and $\underline{\mathbf{M}}$ satisfy Eq. (9.26) suggests that there is a connection between the fundamental solution $\underline{\mathbf{M}}$ and the eigenstructures $\underline{G}$ and κ of $\underline{K}$. This comparison also suggests that $\underline{\mathbf{M}}$ behaves like an exponential function of ζ.

We shall pursue these matters for the remainder of this chapter and, in so doing, we shall uncover results both philosophically profound and numerically useful. These results have been developed over the years by various researchers. Notable historical papers are those of Aronson (1972) and of Waterman (1981). Plass, *et al*. (1973) give a detailed review of the earlier literature. The treatment in this chapter follows unpublished notes of Preisendorfer, which are collected in Preisendorfer (1986).

We first define a general eigenmatrix problem. Recall that in Eq. (8.44) we defined arrays $\underline{\hat{L}}^{\pm}(\zeta;l)$ that were either $1\times m$ if $p = 1$ and $l = 0$, or $1\times(m-1)$ otherwise. In Eq. (9.14) we defined $\underline{\hat{L}}^{\pm}_{p}(\zeta;l)$ as being $1\times n$, or perhaps $1\times M$ if the δ-M phase function approximation is being used. Likewise, $\hat{\mathfrak{t}}(l)$ and $\hat{\rho}(l)$ are defined in Eq. (8.42) as being either $m\times m$ or $(m-1)\times(m-1)$ matrices, for $l = 0$ and $l > 0$, respectively. Similar $n\times n$ or $M\times M$ matrices were defined in Eqs. (9.15) and (9.16).

Let us now define general $1\times q$ arrays

$$\begin{aligned}\underline{\hat{L}}^{\pm}(\zeta) &\equiv [\hat{L}(\zeta;\pm\mu_1),\ \hat{L}(\zeta;\pm\mu_2),\ ...,\ \hat{L}(\zeta;\pm\mu_q)] \\ &\equiv [\hat{L}^{\pm}(\zeta;1),\ \hat{L}^{\pm}(\zeta;2),\ ...,\ \hat{L}^{\pm}(\zeta;q)]\,,\end{aligned} \tag{9.29}$$

and $q\times q$ matrices $\underline{\hat{\tau}}$ and $\underline{\hat{\rho}}$. Here q can be m or $m-1$, n or M, depending on the particular origin of the arrays. It is the general forms of $\underline{\hat{L}}^{\pm}$, $\underline{\hat{\tau}}$ and $\underline{\hat{\rho}}$ that are important, not their size or detailed definitions. We shall therefore omit any arguments like p or l, while retaining the depth argument ζ. With these definitions, *the local interaction equations for source-free, homogeneous water can be written as*

$$\mp\frac{d}{d\zeta}\underline{\hat{L}}^{\mp}(\zeta) = \underline{\hat{L}}^{\mp}(\zeta)\,\underline{\hat{\tau}} + \underline{\hat{L}}^{\pm}(\zeta)\,\underline{\hat{\rho}}\,. \tag{9.30}$$

Note that $\underline{\hat{\tau}}$ and $\underline{\hat{\rho}}$ are now independent of depth. In matrix form, Eq. (9.30) reads

$$\frac{d}{d\zeta}[\underline{\hat{L}}^{-}(\zeta),\ \underline{\hat{L}}^{+}(\zeta)] = [\underline{\hat{L}}^{-}(\zeta),\ \underline{\hat{L}}^{+}(\zeta)]\begin{bmatrix}-\underline{\hat{\tau}} & \underline{\hat{\rho}} \\ -\underline{\hat{\rho}} & \underline{\hat{\tau}}\end{bmatrix},$$

or

$$\frac{d}{d\zeta}\underline{\hat{L}}(\zeta) = \underline{\hat{L}}(\zeta)\,\underline{K}\,. \tag{9.31}$$

In Eq. (9.31) we have defined the $1\times 2q$ array

$$\underline{\hat{L}}(\zeta) \equiv [\underline{\hat{L}}^{-}(\zeta),\ \underline{\hat{L}}^{+}(\zeta)] \tag{9.32}$$

and the $2q\times 2q$ local transfer matrix

$$\underline{K} \equiv \begin{bmatrix}-\underline{\hat{\tau}} & \underline{\hat{\rho}} \\ -\underline{\hat{\rho}} & \underline{\hat{\tau}}\end{bmatrix}. \tag{9.33}$$

We are considering here infinitely deep, source-free, homogeneous water bodies $S[w,m]$, so that $0 \le w \le \zeta \le m \le b = \infty$. In addition, we shall *assume* that we know the radiance amplitude $\underline{\hat{L}}(w)$ just below the air-water surface. These assumptions will allow us to concentrate on the essential results, without carrying along the extra mathematical terms associated with internal sources, finite depths, or surface boundary conditions.

9.3 Eigenstructures of the Local Transfer Matrix $\underline{K}$

We have now posed a $2q$-dimensional matrix problem: find the solution $\underline{\hat{L}}(\zeta)$ of Eq. (9.31). Because Eq. (9.31) is a *linear* equation, there should exist a set of $2q$ distinct *basis functions*, such that the general solution of Eq. (9.31) can be written as a linear combination of the basis functions. Moreover, we already have observed in Eq. (9.25) that the general solution should behave with depth like a sum of exponentials.

Natural basis functions for radiance amplitudes

Based on the preceding comments, we *postulate the existence of a set of 2q linearly independent basis functions* of the form

$$B_j^{\pm}(\zeta) = B_j^{\pm}(w) \exp[\kappa_j^{\pm}(\zeta - w)] , \tag{9.34}$$

where $j = 1, ..., q$. Here the $\kappa_j^{\pm}$ are $2q$ distinct, dimensionless, real numbers. The $\kappa_j^{\pm}$ are dimensionless because we are working with dimensionless optical depths ζ and w. In homogeneous water, $\zeta = cz$. Thus, if we wish to work with geometric depth z, we write the exponential in Eq. (9.34) as $\exp[k_j^{\pm}(z - w)]$, where $k_j^{\pm} \equiv c\kappa_j^{\pm}$ has dimensions of m^{-1}. The $\kappa_j^{\pm}$ are *decay* (or growth) *constants associated with the basis functions* $B_j^{\pm}$. They should not be confused with the *diffuse attenuation functions* [K_d, $K(\theta,\phi)$, etc], which can be thought of as decay constants for actual (measurable) irradiances or radiances. The basis functions will prove to be convenient mathematical constructions, but they are *not observable*; that is to say, the $B_j^{\pm}$'s cannot be measured with a radiometric instrument. McCormick and Højerslev (1994) have pointed out problems that can arise if the conceptually distinct κ's and K's are confused. As we shall see, however, the κ's and K's are related.

Note from Eq. (9.34) that

$$\frac{d}{d\zeta} B_j^{\pm}(\zeta) = B_j^{\pm}(w) \exp[\kappa_j^{\pm}(\zeta - w)]\, \kappa_j^{\pm} = B_j^{\pm}(\zeta)\, \kappa_j^{\pm} . \tag{9.35}$$

We can collect these basis functions into arrays, just as in Eqs. (9.29) and (9.32):

$$\underline{B}^{\pm}(\zeta) \equiv [B_1^{\pm}(\zeta), ..., B_q^{\pm}(\zeta)]$$

and

$$\underline{\boldsymbol{B}}(\zeta) \equiv [\underline{\boldsymbol{B}}^{-}(\zeta), \underline{\boldsymbol{B}}^{+}(\zeta)] .$$

In addition, let us define the $q \times q$ *diagonal* matrices

$$\underline{\kappa}^{\pm} \equiv \begin{bmatrix} \kappa_1^{\pm} & 0 & \cdots & 0 \\ 0 & \kappa_2^{\pm} & \cdots & 0 \\ \vdots & \vdots & \ddots & \vdots \\ 0 & 0 & \cdots & \kappa_q^{\pm} \end{bmatrix}, \tag{9.36}$$

and the $2q \times 2q$ diagonal matrix

$$\underline{\kappa} \equiv \begin{bmatrix} \underline{\kappa}^{-} & \underline{0} \\ \underline{0} & \underline{\kappa}^{+} \end{bmatrix}, \tag{9.37}$$

where $\underline{0}$ is the $q \times q$ matrix of zeros. With these definitions, Eq. (9.34) can be written

$$\underline{\boldsymbol{B}}^{\pm}(\zeta) = \underline{\boldsymbol{B}}^{\pm}(w) \exp[\underline{\kappa}^{\pm}(\zeta - w)] \tag{9.38}$$

or

$$\underline{\boldsymbol{B}}(\zeta) = \underline{\boldsymbol{B}}(w) \exp[\underline{\kappa}(\zeta - w)]. \tag{9.39}$$

In such matrix equations, the exponential is defined by

$$\exp[\underline{A}\zeta] \equiv \sum_{i=0}^{\infty} \underline{A}^i \frac{\zeta^i}{i!}, \tag{9.40}$$

where $\underline{A}$ is any square matrix. Note also that

$$\frac{d}{d\zeta} \exp[\underline{A}\zeta] = \exp[\underline{A}\zeta]\underline{A} . \tag{9.41}$$

Likewise, Eq. (9.35) can be written

$$\frac{d}{d\zeta} \underline{\boldsymbol{B}}(\zeta) = \underline{\boldsymbol{B}}(\zeta)\underline{\kappa} . \tag{9.42}$$

We next recall that by hypothesis the general solution $\underline{\hat{\boldsymbol{L}}}(\zeta)$ of Eq. (9.31) can be written as a linear combination of the $2q$ basis functions $\boldsymbol{B}_j^{\pm}$:

$$\hat{\boldsymbol{L}}^{\pm}(\zeta;u) = \sum_{j=1}^{q} \boldsymbol{B}_j^{-}(\zeta) f_j^{-\pm}(u) + \sum_{j=1}^{q} \boldsymbol{B}_j^{+}(\zeta) f_j^{+\pm}(u) , \tag{9.43}$$

where $u = 1, ..., q$ as in Eq. (9.29), and the $f_j^{\pm\pm}(u)$ are coefficients that remain to be determined. These coefficients can be placed in matrix form via

$$\underline{f}_j^{\pm\pm} \equiv [f_j^{\pm\pm}(1), \ ..., \ f_j^{\pm\pm}(q)] .$$

Equation (9.43) then becomes

$$\hat{\underline{L}}^{\pm}(\zeta) = \sum_{j=1}^{q} B_j^{-}(\zeta) \underline{f}_j^{-\pm} + \sum_{j=1}^{q} B_j^{+}(\zeta) \underline{f}_j^{+\pm} .$$

In more compact form we can write

$$[\hat{\underline{L}}^{-}(\zeta), \ \hat{\underline{L}}^{+}(\zeta)] = [\underline{B}^{-}(\zeta), \ \underline{B}^{+}(\zeta)] \begin{bmatrix} \underline{F}^{--} & \underline{F}^{-+} \\ \underline{F}^{+-} & \underline{F}^{++} \end{bmatrix}, \tag{9.44}$$

or

$$\hat{\underline{L}}(\zeta) = \underline{B}(\zeta) \, \underline{F} . \tag{9.45}$$

The $\underline{F}^{\pm\pm}$ arrays are each $q \times q$. They are formed by "stacking up" the $1 \times q$ row vectors $\underline{f}^{\pm\pm}$:

$$\underline{F}^{\pm\pm} \equiv \begin{bmatrix} \underline{f}_1^{\pm\pm} \\ \vdots \\ \underline{f}_q^{\pm\pm} \end{bmatrix} .$$

Note that $\underline{F}^{+-}$ transforms $\underline{B}^{+}(\zeta)$ into $\hat{\underline{L}}^{-}(\zeta)$, and so on. Note also that the mapping $\underline{F}$ is independent of depth, even though it transforms the basis functions at depth ζ into the radiance amplitudes at depth ζ, for any ζ.

Transformation (9.45) can be postulated to go in the reverse direction, i.e., from $\hat{\underline{L}}$ to $\hat{\underline{B}}$, in which case we can write

$$\underline{B}(\zeta) = \hat{\underline{L}}(\zeta) \, \underline{F}^{-1} \equiv \hat{\underline{L}}(\zeta) \, \underline{E} , \tag{9.46}$$

provided that $\underline{F}^{-1}$ exists. Reversing the steps leading from Eq. (9.43), we can decompose Eq. (9.46) to obtain

$$[\underline{B}^{-}(\zeta), \ \underline{B}+(\zeta)] = [\hat{\underline{L}}^{-}(\zeta), \ \hat{\underline{L}}^{+}(\zeta)] \begin{bmatrix} \underline{E}^{--} & \underline{E}^{-+} \\ \underline{E}^{+-} & \underline{E}^{++} \end{bmatrix}, \tag{9.47}$$

or

$$\underline{B}^{\pm}(\zeta) = \sum_{u=1}^{q} \hat{L}(\zeta;u)\,\underline{e}^{-\pm}(u) + \sum_{u=1}^{q} \hat{L}^{+}(\zeta;u)\,\underline{e}^{+\pm}(u)\,, \tag{9.48}$$

or finally

$$B_j^{\pm}(\zeta) = \sum_{u=1}^{q} \hat{L}(\zeta;u)\,e_j^{-\pm}(u) + \sum_{u=1}^{q} \hat{L}^{+}(\zeta;u)\,e_j^{+\pm}(u)\,, \tag{9.49}$$

where $j = 1, ..., q$. Note, however, the difference in running index variables in Eq. (9.49) vs. Eq. (9.43).

The eigenstructure equation

Results (9.34) to (9.49) have all been obtained by hypothesis and definition. We still do not know how to compute $\underline{\kappa}$, $\underline{B}$, or $\underline{F}$. However, combining Eqs. (9.42) and (9.46) gives

$$\frac{d}{d\zeta}\underline{B}(\zeta) = \underline{B}(\zeta)\,\underline{\kappa} = \underline{\hat{L}}(\zeta)\,\underline{E}\,\underline{\kappa}\,.$$

On the other hand, taking the ζ derivative of Eq. (9.46) and using (9.31) gives

$$\frac{d}{d\zeta}\underline{B}(\zeta) = \frac{d}{d\zeta}[\underline{\hat{L}}(\zeta)\,\underline{E}] = [\frac{d}{d\zeta}\underline{\hat{L}}(\zeta)]\,\underline{E} = \underline{\hat{L}}(\zeta)\,\underline{K}\,\underline{E}\,.$$

Equating these two forms of $d\underline{B}/d\zeta$ and noting that $\underline{\hat{L}}(\zeta)$ is arbitrary gives the all-important equation

$$\underline{K}\,\underline{E} = \underline{E}\,\underline{\kappa}\,. \tag{9.50}$$

This equation shows that $\underline{E}$ and $\underline{\kappa}$ are the *eigenstructures*, that is the *eigenvectors* and *eigenvalues*, of $\underline{K}$. If we view the *columns* of $\underline{E}$ as $2q\times1$ vectors

$$\underline{e}_j \equiv \begin{bmatrix} E_{1,j} \\ E_{2,j} \\ \vdots \\ E_{2q,j} \end{bmatrix},$$

and recall that $\underline{\kappa}$ is diagonal, Eq. (9.50) can be written in the customary eigenvector-eigenvalue form

$$\underline{K}\,\underline{e}_j = \kappa_j\,\underline{e}_j \quad \text{for } j = 1, 2, ..., 2q\,. \tag{9.51}$$

Thus the j^{th} eigenvector of $\underline{K}$ forms the j^{th} column of $\underline{E}$, and the associated j^{th} eigenvalue is the corresponding element κ_{jj} of $\underline{\kappa}$. This is the first major result of this section.

Another way to view Eq. (9.50) is to write it as

$$\underline{E}^{-1}\,\underline{K}\,\underline{E} \equiv \underline{F}\,\underline{K}\,\underline{F}^{-1} = \underline{\kappa}\,. \tag{9.52}$$

We then see that $\underline{E}^{-1} = \underline{F}$ *is the matrix that diagonalizes the local transfer matrix* $\underline{K}$.

Eigenrepresentation of the fundamental solution

The connection between the fundamental solution $\underline{\mathbf{M}}(w,\zeta)$ and the eigenstructures of $\underline{K}$ is now easily established. The mapping property (9.27) can be combined with the basis representation (9.45) and Eq. (9.39) to give

$$\begin{aligned}\hat{\underline{L}}(w)\,\underline{\mathbf{M}}(w,\zeta) &= \hat{\underline{L}}(\zeta)\\ &= \underline{B}(\zeta)\,F\\ &= \underline{B}(w)\exp[\underline{\kappa}(\zeta - w)]\,\underline{F}\,.\end{aligned}$$

Now by Eq. (9.46) evaluated at $\zeta = w$, we can replace $\underline{B}(w)$ in the previous equation by $\hat{\underline{L}}(w)\,\underline{E}$ to get

$$\hat{\underline{L}}(w)\,\underline{\mathbf{M}}(w,\zeta) = \hat{\underline{L}}(w)\,\underline{E}\exp[\underline{\kappa}(\zeta - w)]\,\underline{F}\,.$$

Since $\hat{\underline{L}}(w)$ is arbitrary, we immediately conclude that

$$\underline{\mathbf{M}}(w,\zeta) = \underline{E}\exp[\underline{\kappa}(\zeta - w)]\,\underline{F}\,. \tag{9.53}$$

Equation (9.53) shows how *the fundamental solution can be obtained from the eigenstructures of* $\underline{K}$. *This is the second major result of this section.*

We can reduce Eq. (9.53) even further by expanding the exponential and using Eq. (9.52):

$$\begin{aligned}\underline{\mathbf{M}}(w,\zeta) &= \underline{E}\exp[\underline{\kappa}(\zeta - w)]\,\underline{F}\\ &= \underline{E}\left[\sum_{i=0}^{\infty}\underline{\kappa}^{i}\,\frac{(\zeta - w)^{i}}{i!}\right]\underline{E}^{-1}\\ &= \sum_{i=0}^{\infty}(\underline{E}\,\underline{\kappa}\,\underline{E}^{-1})^{i}\,\frac{(\zeta - w)^{i}}{i!}\end{aligned}$$

$$= \sum_{i=0}^{\infty} \underline{\mathbf{K}}^i \frac{(\zeta - w)^i}{i!}$$

$$\underline{\mathbf{M}}(w,\zeta) = \exp[\underline{\mathbf{K}}(\zeta - w)]. \tag{9.54}$$

We thus have an *elegant representation of the fundamental solution as an exponential of the local transfer matrix* $\underline{K}$. Note that for $\zeta = w$ we get just

$$\underline{\mathbf{M}}(w,w) = \underline{I}_{2q}. \tag{9.55}$$

This is precisely the initial condition (8.62) that we used to obtain the fundamental solution $\underline{\mathbf{M}}(w,\zeta)$ by depth integration of the differential equation system (8.61),

$$\frac{d}{d\zeta}\underline{\mathbf{M}}(w,\zeta) = \underline{\mathbf{M}}(w,\zeta)\,\underline{\mathbf{K}}(\zeta). \tag{9.56}$$

In the general case of depth-dependent IOP's, i.e., when $\underline{K}$ is a function of ζ, integration of Eq. (9.56) is the most efficient way to obtain $\underline{\mathbf{M}}(w,\zeta)$. In the special case of constant $\underline{K}$, we also can obtain $\underline{\mathbf{M}}(w,\zeta)$ simply by evaluating exponentials.

Equation (9.54) is convenient for theoretical discussions (see, for example, problem 9.2). However, in numerical computations, Eq. (9.53) is more convenient than (9.54) because the matrix $\underline{\kappa}$ in the exponential is diagonal. For diagonal matrices (only!) we have

$$\exp[\underline{\kappa}(\zeta - w)] = \begin{bmatrix} \exp[\kappa_{11}(\zeta - w)] & 0 & \cdots & 0 \\ 0 & \exp[\kappa_{22}(\zeta - w)] & \cdots & 0 \\ \vdots & \vdots & \ddots & \vdots \\ 0 & 0 & \cdots & \exp[\kappa_{2q,2q}(\zeta - w)] \end{bmatrix}$$

This result makes the numerical evaluation of Eq. (9.53) much easier than the evaluation of Eq. (9.54), which in general can be quite difficult.

9.4 Properties of the Eigenstructures of $\underline{K}$

The symmetries (5.7) of the scattering phase function are responsible for the block-antisymmetric form of the local transfer matrix $\underline{K}$. This special structure of $\underline{K}$ in turn leads to certain symmetries in its eigenvectors $\underline{e}_j$ and eigenvalues κ_j, which we now investigate.

Decomposing the radiances into downward (+) upward (−) parts already has led us to write the $2q\times 2q$ matrix of eigenvectors, $\underline{E}$, as [recall Eqs. (9.47) and (9.51)]

$$\underline{E} = \begin{bmatrix} \underline{E}^{--} & \underline{E}^{-+} \\ \underline{E}^{+-} & \underline{E}^{++} \end{bmatrix} = \left[\underline{e}_1, \ ..., \ \underline{e}_q, \ \underline{e}_{q+1}, \ ..., \ \underline{e}_{2q} \right]. \tag{9.57}$$

This equation suggests that we partition each of the $2q\times 1$ eigenvectors $\underline{e}_j$ into two $q\times 1$ vectors according to the patterns

$$\underline{e}_j = \begin{bmatrix} \underline{e}_j^{--} \\ \underline{e}_j^{+-} \end{bmatrix} \tag{9.58a}$$

for $j = 1, ..., q;$ and

$$\underline{e}_j = \begin{bmatrix} \underline{e}_j^{-+} \\ \underline{e}_j^{++} \end{bmatrix} \tag{9.58a}$$

for $j = q+1, ..., 2q$. Here the $\underline{e}_j^{\pm\pm}$ are each qx1 arrays.

Reversal property of the eigenstructures

Now suppose that $\underline{e}_j$ is a $2q\times 1$ vector of the form of Eq. (9.58a). The *reverse* of $\underline{e}_j$ is defined as

$$\underline{e}_j^{\mathrm{R}} \equiv \begin{bmatrix} \underline{e}_j^{+-} \\ \underline{e}_j^{--} \end{bmatrix} = \begin{bmatrix} \underline{0}_q & \underline{I}_q \\ \underline{I}_q & \underline{0}_q \end{bmatrix} \begin{bmatrix} \underline{e}_j^{--} \\ \underline{e}_j^{+-} \end{bmatrix} \equiv \underline{Q}\, \underline{e}_j \, . \tag{9.59}$$

Here $\underline{Q}$ is the $2q\times 2q$ *reversal matrix*. Observe by straightforward computation that

$$\underline{Q}^2 = \underline{I}_{2q} \tag{9.60}$$

and

$$\underline{Q}\,\underline{K} = -\underline{K}\,\underline{Q}, \tag{9.61}$$

which implies that

$$\underline{Q}\,\underline{K}\,\underline{Q} = -\underline{K}. \tag{9.62}$$

Now let $\underline{e}_j$ be the eigenvector of $\underline{K}$ associated with eigenvalue $\underline{\kappa}_j$, $j = 1, ..., q$. Then by definition

$$\underline{\boldsymbol{K}}\,\underline{\boldsymbol{e}}_j = \kappa_j \underline{\boldsymbol{e}}_j .$$

Multiplying this equation on the left by $\underline{\boldsymbol{Q}}$ and using Eq. (9.60) gives

$$\underline{\boldsymbol{Q}}\,\underline{\boldsymbol{K}}\,\underline{\boldsymbol{Q}}^2\,\underline{\boldsymbol{e}}_j = \kappa_j \underline{\boldsymbol{Q}}\,\underline{\boldsymbol{e}}_j ,$$

which by Eqs. (9.59) and (9.62) reduces to

$$\underline{\boldsymbol{K}}\,\underline{\boldsymbol{e}}_j^{\mathrm{R}} = -\kappa_j \underline{\boldsymbol{e}}_j^{\mathrm{R}} . \tag{9.63}$$

Thus we conclude that if $\underline{e}_j$ and κ_j are an eigenstructure of $\underline{K}$, then so are $\underline{\boldsymbol{e}}_j^{\mathrm{R}}$ and $-\kappa_j$. From this, we see that *the eigenvalues of* $\underline{K}$ *come in signed pairs,* $\pm\kappa_j$, $j = 1, ..., q$.

If we re-index the eigenvalues so that $\kappa_{j+q} = -\kappa_j$, $j = 1, ..., q$, then $\underline{\boldsymbol{e}}_{j+q} = \underline{\boldsymbol{e}}_j^{\mathrm{R}}$, $j = 1, ..., q$. Hence, it follows that in Eq. (9.58) we have

$$\begin{aligned} \underline{\boldsymbol{e}}_j^{++} &= \underline{\boldsymbol{e}}_j^{--} \equiv \underline{\boldsymbol{e}}_j^{+} \\ \underline{\boldsymbol{e}}_j^{-+} &= \underline{\boldsymbol{e}}_j^{+-} \equiv \underline{\boldsymbol{e}}_j^{-} . \end{aligned} \tag{9.64}$$

We can therefore simplify the notation of Eq. (9.57) to

$$\underline{\boldsymbol{E}} = \begin{bmatrix} \underline{\boldsymbol{E}}^{+} & \underline{\boldsymbol{E}}^{-} \\ \underline{\boldsymbol{E}}^{-} & \underline{\boldsymbol{E}}^{+} \end{bmatrix} . \tag{9.65}$$

A corresponding notation, $\underline{\boldsymbol{F}}^{++} = \underline{\boldsymbol{F}}^{--} \equiv \underline{\boldsymbol{F}}^{+}$, $\underline{\boldsymbol{F}}^{+-} = \underline{\boldsymbol{F}}^{-+} \equiv \underline{\boldsymbol{F}}^{-}$, can be used in Eq. (9.44).

Uniqueness of the eigenstructures

We have been assuming that the eigenvectors of $\underline{K}$ are linearly independent. Simple physical arguments convince us that our assumption is indeed justified.

Without loss of generality, we can arrange the non-negative eigenvalues κ_j, $j = 1, ..., q$, into ascending order:

$$\kappa_1 \le \kappa_2 \le \ldots \le \kappa_q .$$

Observations show that in optically deep, source-free, homogeneous waters illuminated from the sky, the radiance *eventually* decays exponentially with

increasing depth. This implies that κ_1 must be positive: $\kappa_1 \leq 0$ would imply that the radiance amplitude associated with κ_1 via Eqs. (9.34) and (9.45) would not decay with depth, and hence neither would the radiance.

We next observe that downwelling radiance near the surface [for example, $\boldsymbol{L}^+(w;u)$, $u = 1, ..., q$, in quad-averaged notation] has q degrees of freedom. For example, as the sun rises in the sky, the radiance in each u-quad changes, if all else is held constant. Hence, the full q-dimensionality of the associated amplitude $\hat{\underline{\boldsymbol{L}}}^+(\zeta;u)$ $u = 1, ..., q$, is required to determine the downwelling radiance. This implies that the eigenvalues $\kappa_j, j = 1, ..., q$ are all distinct. We therefore conclude that

$$0 < \kappa_1 < \kappa_2 < ... < \kappa_q .$$

The pairwise distinctness of the eigenvalues implies the linear independence of the associated eigenvectors $\underline{e}_j$, $j = 1, ..., 2q$. The linear independence of the eigenvectors forming $\underline{E}$ in turn guarantees us that $\underline{\boldsymbol{E}}^{-1} \equiv \underline{\boldsymbol{F}}$ exists, as was assumed in writing Eq. (9.52).

Indeed, the decomposition of the radiance into downwelling and upwelling parts, in combination with the above physical arguments, implies that the sets of vectors $\underline{e}_1^+, ..., \underline{e}_q^+$ and $\underline{e}_1^-, ..., \underline{e}_q^-$ are each linearly independent. This guarantees us that $(\underline{\boldsymbol{E}}^+)^{-1}$ and $(\underline{\boldsymbol{E}}^-)^{-1}$ each exist. This last result will prove useful below.

Reduction of the eigenmatrix order

The eigenmatrix symmetries seen in Eq. (9.64) yield an important reduction in the size of the eigenmatrix problem that must be solved in order to determine the eigenstructures of $\underline{K}$. Recalling Eq. (9.64), we can write the 2qx2q eigenmatrix equation as

$$\begin{bmatrix} -\underline{\tau} & \underline{\rho} \\ -\underline{\rho} & \underline{\tau} \end{bmatrix} \begin{bmatrix} \underline{e}_j^+ \\ \underline{e}_j^- \end{bmatrix} = \kappa_j \begin{bmatrix} \underline{e}_j^+ \\ \underline{e}_j^- \end{bmatrix}. \tag{9.66}$$

Expanding Eq. (9.66) gives

$$\begin{aligned} -\underline{\tau}\,\underline{e}_j^+ + \underline{\rho}\,\underline{e}_j^- &= \underline{\kappa}_j\,\underline{e}_j^+ \\ -\underline{\rho}\,\underline{e}_j^+ + \underline{\tau}\,\underline{e}_j^- &= \kappa_j\,\underline{e}_j^- . \end{aligned}$$

Adding and subtracting these two equations gives

$$\underline{\tau}\,(\underline{e}_j^- - \underline{e}_j^+) + \underline{\rho}\,(\underline{e}_j^- - \underline{e}_j^+) = \kappa_j\,(\underline{e}_j^- + \underline{e}_j^+) \tag{9.67a}$$

$$-\underline{\tau}\,(\underline{e}_j^+ + \underline{e}_j^-) + \underline{\rho}\,(\underline{e}_j^+ + \underline{e}_j^-) = \kappa_j\,(\underline{e}_j^+ - \underline{e}_j^-)\,. \tag{9.67b}$$

Solving Eq. (9.67a) for $\underline{e}_j^- + \underline{e}_j^+$ and substituting the result into Eq. (9.67b) gives the $q \times q$ eigenmatrix equation

$$(\underline{\tau} - \underline{\rho})(\underline{\tau} + \underline{\rho})(\underline{e}_j^- - \underline{e}_j^+) = \kappa_j^2\,(\underline{e}_j^- - \underline{e}_j^+)\,. \tag{9.68}$$

We can solve this q-dimensional eigenstructure equation in order to determine its eigenvectors $\underline{e}_j^- - \underline{e}_j^+$ and associated eigenvalues κ_j^2, $j = 1, ..., q$. Equation (9.67a) then gives us $\underline{e}_j^+ + \underline{e}_j^-$. Adding and subtracting $\underline{e}_j^- - \underline{e}_j^+$ and $\underline{e}_j^- + \underline{e}_j^+$, finally yields $\underline{e}_j^-$ and $\underline{e}_j^+$, respectively.

The structure of the $2q \times 2q$ system matrix $\underline{K}$ therefore allows us to determine its eigenvectors and eigenvalues from the eigenstructures of the $q \times q$ matrix $(\underline{\tau}-\underline{\rho})(\underline{\tau}+\underline{\rho})$. This reduction from a $2q$- to a q-dimensional problem represents a significant numerical savings, because the computational costs of finding eigenstructures are roughly proportional to the cube of the matrix order.

9.5 Radiance Reflectance of an Infinitely Deep Water Body

Equation (8.56) expresses the spectral form of the bottom boundary condition (8.11) for a natural water body illuminated only from above:

$$\hat{\underline{L}}^-(m) = \hat{\underline{L}}^+(m)\,\hat{\underline{r}}(m,b)\,, \tag{9.69}$$

where we have momentarily dropped the p and l indices seen in Eq. (8.55). We now have the tools necessary to compute $\hat{\underline{r}}(m,b)$ for a bottom boundary $S[m,b] = S[m,\infty]$ that consists of an infinitely deep layer of homogeneous, source-free water. Such a bottom boundary is usually a good model of the deep ocean below the maximum depth m of interest.

In order to evaluate $\hat{\underline{r}}(m,\infty)$, let us first recall that Eq. (9.69) is just a special case of the downward global interaction principles

$$[\hat{\underline{L}}^-(m),\ \hat{\underline{L}}^+(b)] = [\hat{\underline{L}}^-(b),\ \hat{\underline{L}}^+(m)] \begin{bmatrix} \underline{T}(b,m) & \underline{R}(b,m) \\ \underline{R}(m,b) & \underline{T}(m,b) \end{bmatrix} \tag{9.70}$$

written for slab $S[m,b]$; recall Eqs. (8.70), (7.47) and (7.48). Comparing

Eqs. (9.69) and (9.70) shows that $\hat{\underline{r}}(m,b)$ is the same quantity as $R(m,b)$. Moreover, we learned in Eq. (7.51) how to evaluate the standard operators $T(b,m)$, $R(m,b)$, etc. in terms of the fundamental solution $\underline{\mathbf{M}}(m,b)$, which we once again partition as

$$\underline{\mathbf{M}}(m,b) \equiv \begin{bmatrix} \underline{\mathbf{M}}_{--}(m,b) & \underline{\mathbf{M}}_{-+}(m,b) \\ \underline{\mathbf{M}}_{+-}(m,b) & \underline{\mathbf{M}}_{++}(m,b) \end{bmatrix}. \tag{9.71}$$

The $\underline{\mathbf{M}}_{\pm\pm}(m,b)$ are now $q\times q$ matrices. In parallel to Eq. (7.51) in the two-flow case, we now have

$$\underline{R}(m,b) = -\underline{\mathbf{M}}_{+-}(m,b)\,\underline{\mathbf{M}}_{--}^{-1}(m,b)\,. \tag{9.72}$$

Equation (9.53) shows us how to write the $\underline{\mathbf{M}}_{\pm\pm}(m,b)$ matrices in terms of the eigenstructures of the local transfer matrix $\underline{K}$. Expanding Eq. (9.53) as

$$\begin{bmatrix} \underline{\mathbf{M}}_{--}(m,b) & \underline{\mathbf{M}}_{-+}(m,b) \\ \underline{\mathbf{M}}_{+-}(m,b) & \underline{\mathbf{M}}_{++}(m,b) \end{bmatrix} = \begin{bmatrix} \underline{E}^{+} & \underline{E}^{-} \\ \underline{E}^{-} & \underline{E}^{+} \end{bmatrix} \begin{bmatrix} e^{\underline{\kappa}(b-m)} & \underline{0} \\ \underline{0} & e^{-\underline{\kappa}(b-m)} \end{bmatrix} \begin{bmatrix} \underline{F}^{+} & \underline{F}^{-} \\ \underline{F}^{-} & \underline{F}^{+} \end{bmatrix}$$

gives

$$\underline{\mathbf{M}}_{--}(m,b) = \underline{E}^{+} e^{\underline{\kappa}(b-m)} \underline{F}^{+} + \underline{E}^{-} e^{-\underline{\kappa}(b-m)} \underline{F}^{-}, \tag{9.73a}$$

$$\underline{\mathbf{M}}_{+-}(m,b) = \underline{E}^{-} e^{\underline{\kappa}(b-m)} \underline{F}^{+} + \underline{E}^{+} e^{-\underline{\kappa}(b-m)} \underline{F}^{-}, \tag{9.73b}$$

$$\underline{\mathbf{M}}_{-+}(m,b) = \underline{E}^{+} e^{\underline{\kappa}(b-m)} \underline{F}^{-} - \underline{E}^{-} e^{-\underline{\kappa}(b-m)} \underline{F}^{+}, \tag{9.73c}$$

$$\underline{\mathbf{M}}_{++}(m,b) = \underline{E}^{-} e^{\underline{\kappa}(b-m)} \underline{F}^{-} + \underline{E}^{+} e^{-\underline{\kappa}(b-m)} \underline{F}^{+}. \tag{9.73d}$$

Equations (9.73a) and (9.73b) allow Eq. (9.72) to be written as

$$\begin{aligned} \underline{R}(m,b) = &-\left[\underline{E}^{-} e^{\underline{\kappa}(b-m)} \underline{F}^{+} + \underline{E}^{+} e^{-\underline{\kappa}(b-m)} \underline{F}^{-}\right] \\ &\times \left[\underline{E}^{+} e^{\underline{\kappa}(b-m)} \underline{F}^{+} + \underline{E}^{-} e^{-\underline{\kappa}(b-m)} \underline{F}^{-}\right]^{-1}. \end{aligned} \tag{9.74}$$

Now, let $\underline{R}_{\infty}$ denote the spectral form of the radiance reflectance of an infinitely thick slab $S[m,b] = S[m,\infty]$, that is

$$\underline{R}_{\infty} \equiv \lim_{b\to\infty} \underline{R}(m,b)\,.$$

We can explicitly evaluate this limit using Eq. (9.74), since the eigenstructures $\underline{E}^{\pm}$, $\underline{F}^{\pm}$ and $\underline{\kappa}$ are all independent of depth. Let us rewrite Eq. (9.74) as

$$\begin{aligned} R(m,b) \;=\; & -\underline{E}^{-}\, e^{\underline{\kappa}(b-m)}\, \underline{F}^{+} \\ & \times \left[\underline{I}_q \;+\; (\underline{F}^{+})^{-1}\, e^{-\underline{\kappa}(b-m)}\, (\underline{E}^{-})^{-1}\, \underline{E}^{+}\, e^{-\underline{\kappa}(b-m)}\, \underline{F}^{-}\right] \\ & \times \left[\underline{I}_q \;+\; (\underline{F}^{+})^{-1}\, e^{-\underline{\kappa}(b-m)}\, (\underline{E}^{+})^{-1}\, \underline{E}^{-}\, e^{-\underline{\kappa}(b-m)}\, \underline{F}^{-}\right]^{-1} \\ & \times (\underline{F}^{+})^{-1}\, e^{-\underline{\kappa}(b-m)}\, (\underline{E}^{+})^{-1}\,. \end{aligned} \tag{9.75}$$

Here we have repeatedly used the identity $(\underline{A}\,\underline{B})^{-1} = \underline{B}^{-1}\,\underline{A}^{-1}$, where $\underline{A}$ and $\underline{B}$ are any two invertible matrices.

We now take the limit of Eq. (9.75) as $b \to \infty$. The matrix elements in the second terms in each of the square brackets in Eq. (9.75) approach zero at least as rapidly as

$$\exp[\,-2\kappa_1 (b-m)\,]\,,$$

where we recall that $0 < \kappa_1 < \kappa_i$, $2 \le i \le q$. Thus Eq. (9.75) reduces to

$$\underline{R}_{\infty} = \lim_{b\to\infty} R(m,b) = \lim_{b\to\infty}\left\{-\underline{E}^{-}\, e^{\underline{\kappa}(b-m)}\, \underline{F}^{+}\, [\underline{I}_q]\, [\underline{I}_q]\, (\underline{F}^{+})^{-1}\, e^{-\underline{\kappa}(b-m)}\, (\underline{E}^{+})^{-1}\right\},$$

or

$$\underline{R}_{\infty} = \underline{\hat{r}}(m,\infty) = -\underline{E}^{-}\,(\underline{E}^{+})^{-1}\,. \tag{9.76}$$

This very simple result shows how to determine the bottom boundary spectral reflectance from the eigenvectors of $\underline{K}$.

Application to the quad-averaged bottom boundary condition ▌▌

In this chapter we have been omitting the p and l indices in various quantities, for purposes of simplicity of notation. We now pause to consider the details of the use of Eq. (9.76) in the context of the quad-averaged equations of Chapter 8.

We first recall from Eq. (8.42) that $\hat{\underline{\tau}}$ and $\hat{\underline{\rho}}$ are $m\times m$ matrices if $l = 0$, and $(m-1)\times(m-1)$ matrices if $l = 1, 2, \ldots, n$. In Chapter 8 we were able to gloss over the different sizes of the $\hat{\underline{\tau}}$ and $\hat{\underline{\rho}}$ arrays simply by appending a last row and last column of zeros to $\hat{\underline{\tau}}$ and $\hat{\underline{\rho}}$ when $l > 0$, and by appending zero elements to the amplitude array $\hat{\underline{L}}^{+}(\zeta;l)$ when $l \ne 0$ or when $l = 0$ and $p = 2$; recall Eqs. (8.44) and (8.46). However, when using

$\hat{\underline{\tau}}$ and $\hat{\underline{\rho}}$ to form a local transfer matrix $\underline{K}$ for homogeneous water, we must use the properly dimensioned $\hat{\underline{\tau}}$ and $\hat{\underline{\rho}}$, because a last row or column of zeros would make $\underline{K}$ singular. We therefore note that the local transfer matrix $\underline{K}(l)$ is $2m\times 2m$ if $l = 0$, and $2(m-1)\times 2(m-1)$ if $l \neq 0$. This means that $\underline{E}^{+}$ and $\underline{E}^{-}$ are $m\times m$ if $l = 0$, and $(m-1)\times(m-1)$ if $l \neq 0$.

To be specific, then, $\hat{\underline{r}}_p(m,\infty;l)$ is defined as follows:

for $l = 0$:

$$\hat{\underline{r}}_1(m,\infty;0) = \underline{E}^{-}(0)\,[\underline{E}^{+}(0)]^{-1} \quad \text{is } m\times m$$

$$\hat{\underline{r}}_2(m,\infty;0) = \underline{0}_{m\times m} \quad \text{by Eq. (8.57b)}$$

for $l \neq 0$:

$$\hat{\underline{r}}_1(m,\infty;l) = \underline{E}^{-}(l)\,[\underline{E}^{+}(l)]^{-1} \quad \text{is } (m-1)\times(m-1)$$

$$\hat{\underline{r}}_2(m,\infty;l) = \hat{\underline{r}}_1(m,\infty;l) \quad \text{if } l = 1, 2, \ldots, n-1$$

$$\hat{\underline{r}}_2(m,\infty;n) = \underline{0}_{(m-1)\times(m-1)} \quad \text{if } l = n, \text{ by Eq. (8.57b).}$$

In contrast to the case of a Lambertian reflector, the infinite slab has $\hat{\underline{r}}_p$ non-zero when $l > 0$. It is therefore necessary to set up and solve the eigenmatrix equation

$$\underline{K}(l)\,\underline{E}(l) = \underline{E}(l)\,\underline{\kappa}(l)$$

for each l-mode. This is computationally quite reasonable to do. The $\hat{\underline{r}}_p(m,\infty;l)$ so obtained are then ready for use in Eq. (8.94) as initial conditions for the Riccati equation integrations.

Should we wish to recover the actual quad-averaged radiance reflectances of an infinitely deep water body, we return to Eq. (8.54):

$$r(m,\infty;r,s\to u,v) = \sum_{l=0}^{n} \hat{r}(m,\infty;r,u|l)\cos l(\phi_s - \phi_v)\,.$$

The matrix elements $\hat{r}(m,\infty;r,u|l)$ are extracted from the $\hat{\underline{r}}(m,\infty;l)$ arrays by using Eq. (8.57).

Note, that this $\underline{r}(m,\infty)$ is the reflectance of a *bare slab* $S[m,\infty]$; no air-water boundary effects are included. However, the reader who has mastered the concepts of Chapter 7 can easily show (see problem 9.5) that the reflectance of the entire water body, including effects of the air-water surface $S[a,w]$, is

$$\underline{R}(a,\infty) = \underline{r}(a,w) + \underline{t}(a,w)\left[\underline{I} - \underline{R}_\infty \underline{r}(w,a)\right]^{-1} \underline{R}_\infty \underline{t}(w,a)\,. \tag{9.77}$$

Here we have divided the water body into the surface plus the water: $S[a,\infty] = S[a,w] \cup S[w,\infty]$, where $m = w$ in the computation of $\underline{R}_\infty$. The four surface transfer matrices are computable by the methods of Chapter 4.

9.6 The Asymptotic Radiance Distribution

Observations show that deep in homogeneous, source-free waters, radiance distributions approach a *shape* $L_\infty(\theta)$ that depends only as the IOP's. Moreover, the radiance distribution at depth decays in magnitude *exactly exponentially* with a decay rate k_∞ that, once again, depends only on the IOP's. We already have mentioned this fact in Section 5.8; recall Eq. (5.34).

Hypotheses regarding the existence of such an *asymptotic radiance distribution*, or *characteristic diffuse light field*, can be traced back at least to Shuleikin (1933) and Whitney (1941). Preisendorfer (1959; see also *H.O. V*, Section 10.5) took the first careful look at the mathematical requirements for the existence of an asymptotic radiance distribution. Højerslev and Zaneveld (1977) gave the first rigorous mathematical proof that $L_\infty(\theta)$ and k_∞ exist for any physically realistic phase function and single-scattering albedo [see Supplementary Note 12]. The eigenmatrix formalism gives us a straightforward means to compute the shape and decay rate of the asymptotic radiance distribution for a given set of IOP's.

Existence and computation of the asymptotic radiance distribution

Let us begin with the mapping property (9.27) and expand the fundamental solution $\underline{\mathbf{M}}(w,\zeta)$ as in Eq. (9.71):

$$[\hat{\underline{L}}^-(\zeta),\ \hat{\underline{L}}^+(\zeta)] = [\hat{\underline{L}}^-(w),\ \hat{\underline{L}}^+(w)] \begin{bmatrix} \underline{\mathbf{M}}_{--}(w,\zeta) & \underline{\mathbf{M}}_{-+}(w,\zeta) \\ \underline{\mathbf{M}}_{+-}(w,\zeta) & \underline{\mathbf{M}}_{++}(w,\zeta) \end{bmatrix}. \tag{9.78}$$

Equation (9.73) gives the $\underline{\mathbf{M}}_{\pm\pm}(w,\zeta)$ in terms of the eigenstructures of $\underline{K}$. Substituting Eq. (9.73) into (9.78), carrying out the matrix multiplications, and grouping terms gives

$$[\hat{\underline{L}}^{-}(\zeta),\ \hat{\underline{L}}^{+}(\zeta)] = \begin{bmatrix} \underline{a}^{+}(w)\, e^{\underline{K}(\zeta - w)}\, \underline{F}^{+} + \underline{a}^{-}(w)\, e^{-\underline{K}(\zeta - w)}\, \underline{F}^{-}, \\ \underline{a}^{+}(w)\, e^{\underline{K}(\zeta - w)}\, \underline{F}^{-} + \underline{a}^{-}(w)\, e^{-\underline{K}(\zeta - w)}\, \underline{F}^{+} \end{bmatrix}, \tag{9.79}$$

where $\underline{a}^{+}(w)$ and $\underline{a}^{-}(w)$ are $1 \times q$ arrays defined by

$$\underline{a}^{+}(w) \equiv \hat{\underline{L}}^{-}(w)\, \underline{E}^{+} + \hat{\underline{L}}^{+}(w)\, \underline{E}^{-} \tag{9.80a}$$

$$\underline{a}^{-}(w) \equiv \hat{\underline{L}}^{-}(w)\, \underline{E}^{-} + \hat{\underline{L}}^{+}(w)\, \underline{E}^{+}. \tag{9.80b}$$

We can think of $\underline{a}^{\pm}(w)$ as being initial conditions at depth w, which are to be used in determining the radiance amplitudes $\hat{\underline{L}}^{\pm}(\zeta)$ at any depth ζ. As we saw illustrated in Fig. (5.3), radiance can increase or decrease with depth near the water surface, hence the need for both growing and decaying exponentials in Eq. (9.79).

Now let us examine the behavior of Eq. (9.79) as $\zeta \to \infty$. We have just seen that Eq. (9.76) relates $\underline{E}^{-}$ and $\underline{E}^{+}$ in the limit $\zeta \to \infty$,

$$\underline{E}^{-} = -\underline{R}_{\infty} \underline{E}^{+},$$

and we recall from Eq. (9.69) that $\underline{R}_{\infty}$ simply reflects downwelling into upwelling radiance:

$$\hat{\underline{L}}^{-}(w) = \hat{\underline{L}}^{+}(w)\, \underline{R}_{\infty}.$$

(Here we regard $S[w,\infty]$ as the region described by $\underline{R}_{\infty}$.)

At great depths, Eq. (9.80a) then reduces to[1]

$$\underline{a}^{+}(w) = \left[\hat{\underline{L}}^{+}(w)\, \underline{R}_{\infty}\right] \underline{E}^{+} + \hat{\underline{L}}^{+}(w) \left[-\underline{R}_{\infty} \underline{E}^{+}\right] = \underline{0}_{1 \times q},$$

whereas Eq. (9.80b) becomes

$$\underline{a}^{-}(w) = \left[\hat{\underline{L}}^{+}(w)\, \underline{R}_{\infty}\right]\left[-\underline{R}_{\infty} \underline{E}^{+}\right] + \hat{\underline{L}}^{+}(w)\, \underline{E}^{+} = \hat{\underline{L}}^{+}(w) \left[\underline{I} - \underline{R}_{\infty}^{2}\right] \underline{E}^{+} \neq \underline{0}_{1 \times q}.$$

Radiance amplitudes at great depth therefore have the form

$$\hat{\underline{L}}^{\mp}(\zeta) \underset{\zeta \to \infty}{\to} \underline{a}^{-}(w)\, e^{-\underline{K}(\zeta - w)}\, \underline{F}^{\mp}. \tag{9.81}$$

---

[1]The $\underline{a}^{\pm}(w)$ depend implicitly on ζ, as can be seen for example by writing $\hat{\underline{L}}^{-}(w) = \hat{\underline{L}}^{+}(w)\, \underline{R}(w,\zeta) + \hat{\underline{L}}^{-}(\zeta)\, \underline{T}(\zeta,w)$ before letting $\zeta \to \infty$ to get $\underline{R}(w,\zeta) \to \underline{R}_{\infty}$, $\underline{T}(\zeta,w) \to \underline{0}$.

Equation (9.81) is the mathematical statement that *at sufficiently large depths, the radiance always decreases with increasing depth.*

Let us now remember that an equation like (9.81) holds for each l-mode, $l = 0, 1, ..., n$ in the radiance amplitude decomposition. We therefore should index each quantity by l, i.e., $\underline{\boldsymbol{a}}^{-}(w;l)$, $\underline{\boldsymbol{\kappa}}(l)$, and $\underline{\boldsymbol{F}}^{\mp}(l)$. For each l value we always order the eigenvalues as $0 < \kappa_1(l) < \kappa_2(l) < ... < \kappa_q(l)$. Now it also turns out that $\kappa_1(0) < \kappa_1(l)$ for all $l = 1, ..., n$. Physically this reflects the fact that asymmetries and fine details of the radiance distribution near the surface disappear with depth more quickly than the 0-mode, or ϕ-averaged, radiance. Thus in Eq. (9.81) the slowest decaying matrix elements are those associated with $\exp[-\kappa_1(0)(\zeta - w)]$. Equation (9.81) written in component from for $l = 0$ is

$$\hat{L}^{\mp}(\zeta;u;0) = \sum_{v=1}^{q} a_v^{-}(w;0) \exp[-\kappa_v(0)(\zeta - w)] F_{v,u}^{\mp}(0) ,$$

for $u = 1, 2, ..., q$; $q = m$ in the quad-averaged formalism of Chapter 8. If we multiply each side of this equation by $\exp[\kappa_1(0)(\zeta - w)]$ and take the limit as $\zeta \to \infty$, all of the terms for $v > 1$ will go to zero because $\kappa_v(0) > \kappa_1(0)$ for $v > 1$. We thus have left just

$$L_{\infty}^{\mp}(u) = \lim_{\zeta \to \infty} \hat{L}^{\mp}(\zeta;u;0) \exp[\kappa_1(0)(\zeta - w)] = a_1^{-}(w;0) F_{1,u}^{\mp}(0) . \qquad (9.82)$$

Now define the 1x2q array

$$\underline{L}_{\infty} \equiv [\underline{L}_{\infty}^{-}, \underline{L}_{\infty}^{+}] ,$$

where

$$\underline{L}_{\infty}^{\pm} \equiv \left[L_{\infty}^{\pm}(1), ..., L_{\infty}^{\pm}(q) \right] .$$

This $\underline{L}_{\infty}$, or any scalar multiple thereof, is called the *asymptotic radiance distribution*. Note that $\underline{L}_{\infty}$ *is defined by the $l = 0$ cosine radiance amplitudes*; recall that the sine amplitudes are always zero for $l = 0$ (hence we can omit the $p = 1$ or 2 index in the above equations). Because we are dealing with $l = 0$ cosine amplitudes, the amplitudes are just the azimuthally averaged radiances for the various μ_u-bands. Thus $\underline{L}_{\infty}$ depends only on the polar angle θ (or μ) and not on the azimuthal angle ϕ.

Equation (9.82) shows how $\underline{L}_{\infty}$ is easily obtained from the eigenstructures of $\underline{K}(0)$. After finding the eigenvectors $\underline{E}$, we compute $\underline{F} = \underline{E}^{-1}$, and then pick off the elements of the first row of $\underline{F}$, where $\underline{F}$ is partitioned in the manner seen for $\underline{E}$ in Eq. (9.65). Since only the shape of $\underline{L}_{\infty}$ is relevant, it is customary to normalize $\underline{L}_{\infty}$ so that its largest element is

one. In natural waters, this is always the $\boldsymbol{L}_\infty^+(q)$ element, which gives the relative amount of radiance heading into the nadir polar cap. Note that since $\underline{L}_\infty$ is determined only by the IOP's contained in $\underline{K}(0)$, *the asymptotic radiance distribution is itself an inherent optical property*.

We also have just seen that the rate of decay with optical depth of the asymptotic radiance distribution is $\boldsymbol{\kappa}_\infty \equiv \boldsymbol{\kappa}_1(0)$. This decay rate can be expressed in dimensional form as

$$k_\infty \equiv c\boldsymbol{\kappa}_\infty = c\boldsymbol{\kappa}_1(0) \qquad (\mathrm{m}^{-1}), \tag{9.83}$$

where c is the beam attenuation coefficient.

Since each u-component (or direction θ) of $\boldsymbol{L}_\infty^\pm(u)$ in Eq. (9.82) decays at the same rate, we see that *the radiance diffuse attenuation functions $K(z;\theta,\phi)$, which generally differ near the surface, all approach the same value k_∞ at great depth*. This is the connection between diffuse attenuation functions and basis-function decay constants alluded to at the beginning of Section 9.3.

Asymptotic behavior of apparent optical properties

It should be noted that Eq. (9.82) shows that *the directional and depth dependencies of the radiance distribution decouple at great depths*. That is to say,

$$L(z;\theta,\phi) \underset{z\to\infty}{\to} L_\infty(\theta)\exp(-k_\infty z)\,. \tag{9.84}$$

This in turn implies that *all irradiances decay in the asymptotic regime at the same rate as the radiance*. For example,

$$\begin{aligned}\lim_{z\to\infty} E_\mathrm{d}(z) &= \int_0^{2\pi}\int_0^1 L_\infty(\mu)\exp(-k_\infty z)\,\mu\,d\mu\,d\phi \\ &= \left[2\pi\int_0^1 L_\infty(\mu)\,\mu\,d\mu\,d\phi\right]\exp(-k_\infty z) \equiv E_\mathrm{d}(\infty)\exp(-k_\infty z)\,.\end{aligned} \tag{9.85}$$

We can compute corresponding values for E_u, E_od, and E_ou. Clearly, each of these irradiances has the same asymptotic K-function, namely k_∞.

Using these asymptotic irradiances, we can compute asymptotic values for any apparent optical property. For example, we have

$$\bar{\mu}_d(\infty) \equiv \frac{E_d(\infty)}{E_{od}(\infty)} \qquad \bar{\mu}_u(\infty) \equiv \frac{E_u(\infty)}{E_{ou}(\infty)}$$
$$\bar{\mu}(\infty) \equiv \frac{E_d(\infty) - E_u(\infty)}{E_o(\infty)} \qquad R(\infty) \equiv \frac{E_u(\infty)}{E_d(\infty)}. \tag{9.86}$$

Note that any normalization factor in $L_\infty(\theta)$ divides out when computing AOP's.

Some of the relations among AOP's take on particularly simple forms in the asymptotic regime. Recall, for example, Eq. (5.68):

$$\bar{\mu} = \frac{a(1-R)}{K_d - R K_u},$$

which holds for any depth in source-free (but possibly inhomogeneous) water. At great depth, $K_d = K_u = k_\infty$, and this equation simplifies to just

$$\bar{\mu}(\infty) = \frac{a}{k_\infty}.$$

Because the asymptotic radiance L_∞ is determined solely by the IOP's, it follows that any quantity computed from L_∞ is also in IOP. We therefore see that *the apparent optical properties all become inherent optical properties in the asymptotic regime*. The K's, $\bar{\mu}$'s, R and their ilk, which are influenced by boundary conditions near the water surface, all approach values at depth that are independent of the boundary conditions.

Dependence of asymptotic values on inherent optical properties

The two asymptotic properties L_∞ and κ_∞ are determined solely by the IOP's ω_o and $\tilde{\beta}$. Numerical solution of the $l = 0$ eigenmatrix equation as described above enables us to investigate the dependencies of L_∞ and κ_∞ on the IOP's.

Figure 9.2 shows how κ_∞ depends on ω_o for three phase functions. The dotted line is for the pure water phase function $\tilde{\beta}_w$ of Eq. (3.30); the dashed line is for the Henyey-Greenstein phase function $\tilde{\beta}_{HG}$ of Eq. (3.34) with an asymmetry parameter $g = 0.7$; and the solid line is for the particle phase function $\tilde{\beta}_p$ of Table 3.10. The squares show experimental data taken in laboratory suspensions containing milk (Timofeeva and Gorobetz, 1967). The fat globules in milk are large ($>>\lambda$), efficient scatterers, which explains the similarity between the milk solution and particle-laden natural waters.

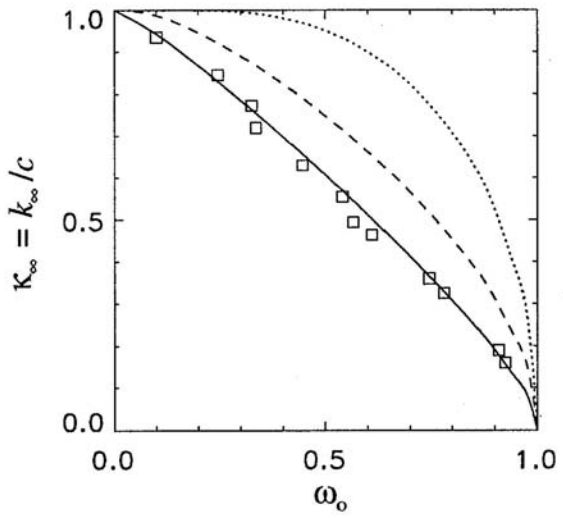

Fig. 9.2. Dependence of κ_∞ on ω_o for selected phase functions. The solid line is for $\tilde{\beta}_p$, the dashed line is for $\tilde{\beta}_{HG}$, and the dotted line is for $\tilde{\beta}_w$, as discussed in the text. The squares are the data of Timofeeva and Gorobetz (1967).

Figure 9.3 shows the shape of $L_\infty(\theta)$ as a function of ω_o for the particle phase function $\tilde{\beta}_p$; all values are normalized to one. The viewing angle θ_v is the angle in which an underwater observer would look in order to see photons traveling in direction $\theta = 180° - \theta_v$; θ_v and θ are both measured from the $+z$, or nadir, direction. Thus, $\theta_v = 180°$ corresponds to looking toward the zenith and seeing photons heading straight down (θ=0). As we would expect, in highly scattering water (large ω_o) the upwelling radiance is relatively much greater than in weakly scattering water (small ω_o). Corresponding curves for the Rayleigh phase function can be seen in Kattawar and Plass (1976). Prieur and Morel (1971) show such curves as a function of the relative contributions by molecular and particle scattering, i.e., for phase functions that are in between $\tilde{\beta}_w$ and $\tilde{\beta}_p$.

Figure 9.4 shows the asymptotic mean cosines and irradiance reflectance computed as in Eqs. (9.85) and (9.86). The quantities are displayed on the same format used in Fig. 9.2: a solid line for $\tilde{\beta}_p$, a dashed line for $\tilde{\beta}_{HG}$, and a dotted line for $\tilde{\beta}_w$. We shall leave it as an exercise to explain the behavior of the curves in Fig. 9.4 in terms of the shapes of the phase functions and of the relative contributions of absorption and scattering to the total attenuation.

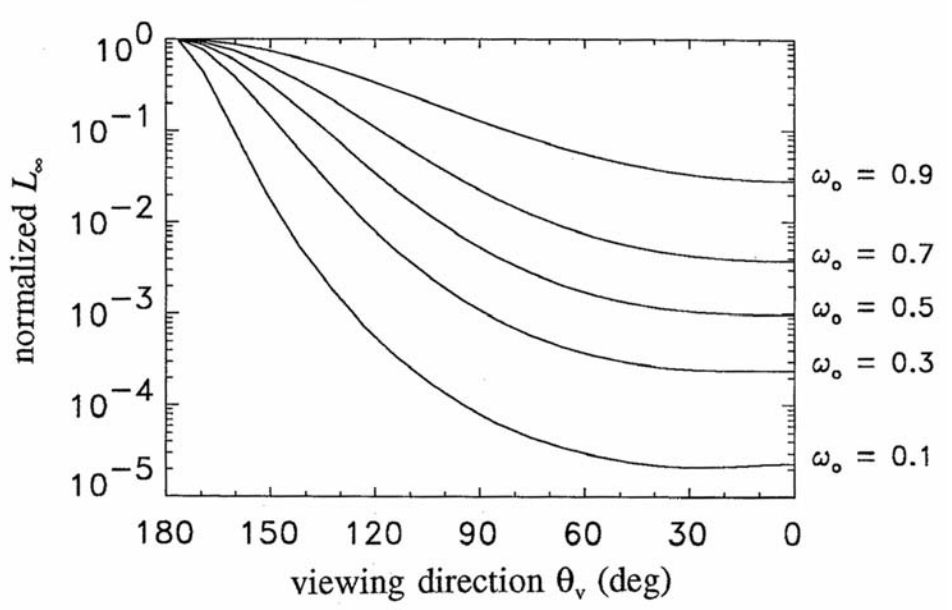

Fig. 9.3. Shape of the asymptotic radiance distribution L_∞ as a function of ω_o, for the particle phase function $\tilde{\beta}_p$. The viewing angle θ_v is $180° - \theta$, as discussed in the text.

Rate of approach to asymptotic values

We have seen that asymptotic values are determined solely by the IOP's of a homogeneous water body. However, in our theoretical discussions above we have said nothing about *how quickly* a given quantity approaches its asymptotic value. The reason is that *the rate of approach to an asymptotic value depends both on the IOP's and on the boundary conditions*.

We can best illustrate this point with a few numerically generated examples. In Section 11.1 we shall examine predictions made by various Monte Carlo, invariant imbedding, and discrete-ordinates numerical models. In so doing, we shall convince ourselves (as is done in Mobley, *et al.*, 1993) that the models all correctly compute underwater radiance distributions, given the IOP's, sea state, and incident sky radiance. For the moment, though, let us assume that the algorithm developed in Chapter 8 correctly computes $L(\zeta;\theta,\phi)$, from which

$$K(\zeta;\theta,\phi) \equiv -\frac{1}{L(\zeta;\theta,\phi)}\frac{dL(\zeta;\theta,\phi)}{d\zeta} = \frac{K(z;\theta,\phi)}{c}$$

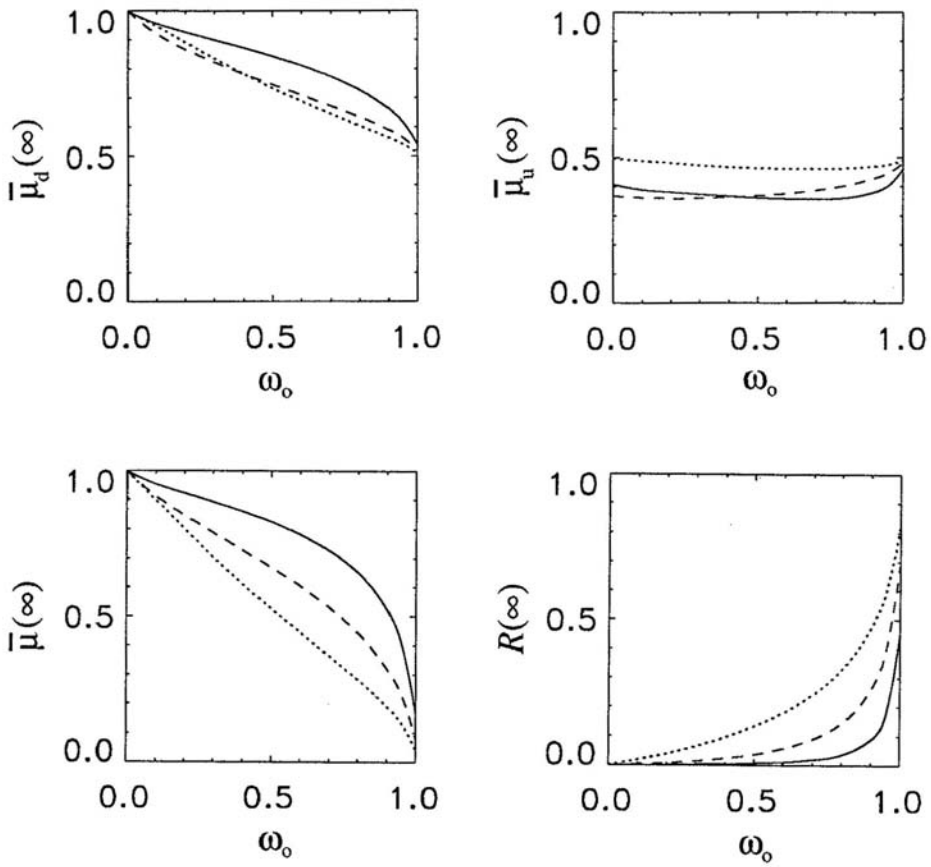

Fig. 9.4. Asymptotic values of the mean cosines and of the irradiance reflectance, as a function of ω_o, for various phase functions. The solid, dashed, and dotted lines correspond to those of Fig. 9.2.

and the various irradiance K-functions can be computed. Note that $K(\zeta;\theta,\phi)$ is a dimensionless "optical depth K-function;" $K(z;\theta,\phi)$ is the customary dimensional K-function with units of m^{-1}.

We consider first a homogeneous, source-free, infinitely deep water body described by the particle phase function $\tilde{\beta}_p$ of Figure 3.13 and by $\omega_o = 0.8$. Table 3.11 shows that such water might be characteristic of a turbid harbor at green wavelengths. The air-water surface is taken to be level. The incident radiance is generated by a point sun at a zenith angle of $\theta_s = 57°$; the sky is otherwise black.

The algorithm of Figs. 8.1 and 8.2 was used to compute $L(\zeta;\theta,\phi)$ throughout the region $S[w,m] = S[0,50]$. Figure 9.5(a) shows the depth

behavior of various K-functions computed from $L(\zeta;\theta,\phi)$. The solid lines are K_d, K_u, and K_o; the two dash-dot lines are radiance $K(\theta,\phi)$'s for photons heading in the nadir and zenith directions [i.e., $K(0°,\cdot)$ and $K(180°,\cdot)$]; and the three dash-dot-dot-dot lines are radiance K's for horizontal directions toward, at right angles to, and away from the sun, i.e., for $(\theta,\phi) = (90°,0°)$, $(90°,90°)$ and $(90°,180°)$. The K-functions vary greatly near the water surface. Even at $\zeta = 5$ optical depths the spread is from $K(0°,\cdot) = 0.127$ to $K(90°,180°) = 0.402$. However, by $\zeta = 50$ the K's have all converged to within ±0.2% of the asymptotic value $k_\infty = 0.310$, which was computed by the eigenmatrix method described above.

Figure 9.5(b) shows the results if we repeat the above numerical simulation using the cardioidal distribution of problem 1.5 for the incident sky radiance. We now see that the various K's approach k_∞ much more quickly than in Fig. 9.5(a): all K's are now within 0.2% of k_∞ by 15 optical depths. The reason for the difference is that the cardioidal sky radiance distribution gives an $L(w;\theta,\phi)$ that is much closer in shape to $L_\infty(\theta)$ than does the collimated radiance of Fig. 9.5(a). Thus, $L(w;\theta,\phi)$ is already well on its way to $L_\infty(\theta)$, and less depth is required to finish getting "near" to the asymptotic distribution. Indeed, we can imaging choosing just the right incident sky radiance $L^+(a;\theta,\phi)$ so that after transmission through the surface and solution of the RTE, we would find $L(w;\theta,\phi) = L_\infty(\theta)$. In this case, all quantities would have their asymptotic values throughout the water column.

The rate of approach to asymptotic values also depends on the IOP's. In Fig. 9.6(a) we show exactly the same situation as in Fig. 9.5(a), except that now $\omega_o = 0.2$. Tables 3.5 and 3.11 show that this ω_o corresponds to very clear ocean water at blue wavelengths. Figure 9.6(b) likewise corresponds to Fig. 9.5(b).

Comparison of Figs. 9.5 and 9.6 shows that in the "high absorption" ($\omega_o = 0.2$) case, the K's approach their asymptotic value, $k_\infty = 0.874$, more slowly than in the "high scattering" ($\omega_o = 0.8$) case. The physical reason is that *scattering is required to redirect the initial photon directions towards the asymptotic angular distribution*. In highly scattering waters this redirection is accomplished relatively quickly. In highly absorbing waters, the light field rapidly decreases in magnitude with depth because of absorption, but it requires a relatively long time for the angular photon distribution to be changed by scattering. The concept of an asymptotic distribution breaks down for $\omega_o = 0$, the case of absorption only; hence k_∞ is undefined for $\omega_o = 0$. In Section 11.2 we shall look at the radiance distributions from which Figs. 9.5(a) and 9.5(b) were produced.

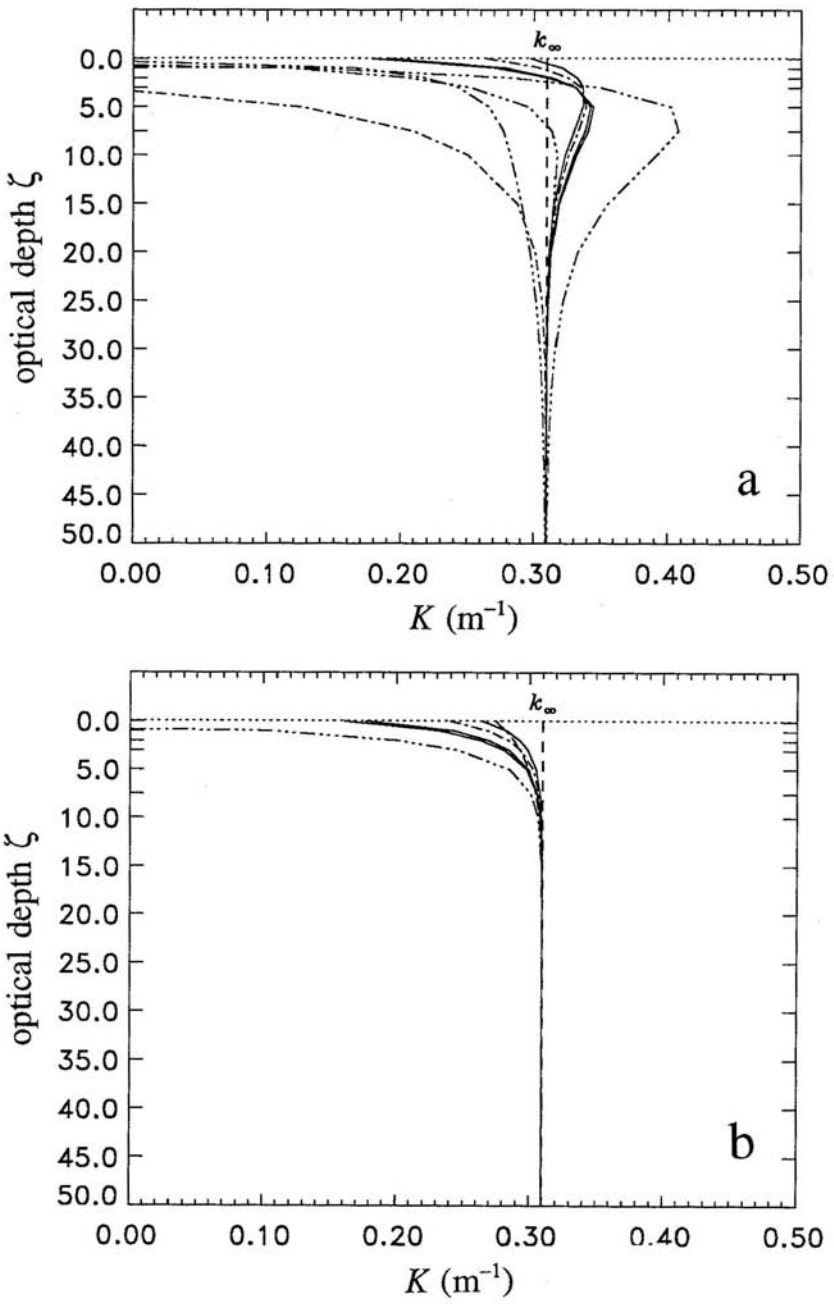

Fig. 9.5. Depth dependence of selected K-functions for highly scattering water ($\omega_o = 0.8$) and different sky lighting conditions. Panel (a) is for the sun at a zenith angle of 57° in a black sky; panel (b) is for a cardioidal sky radiance distribution.

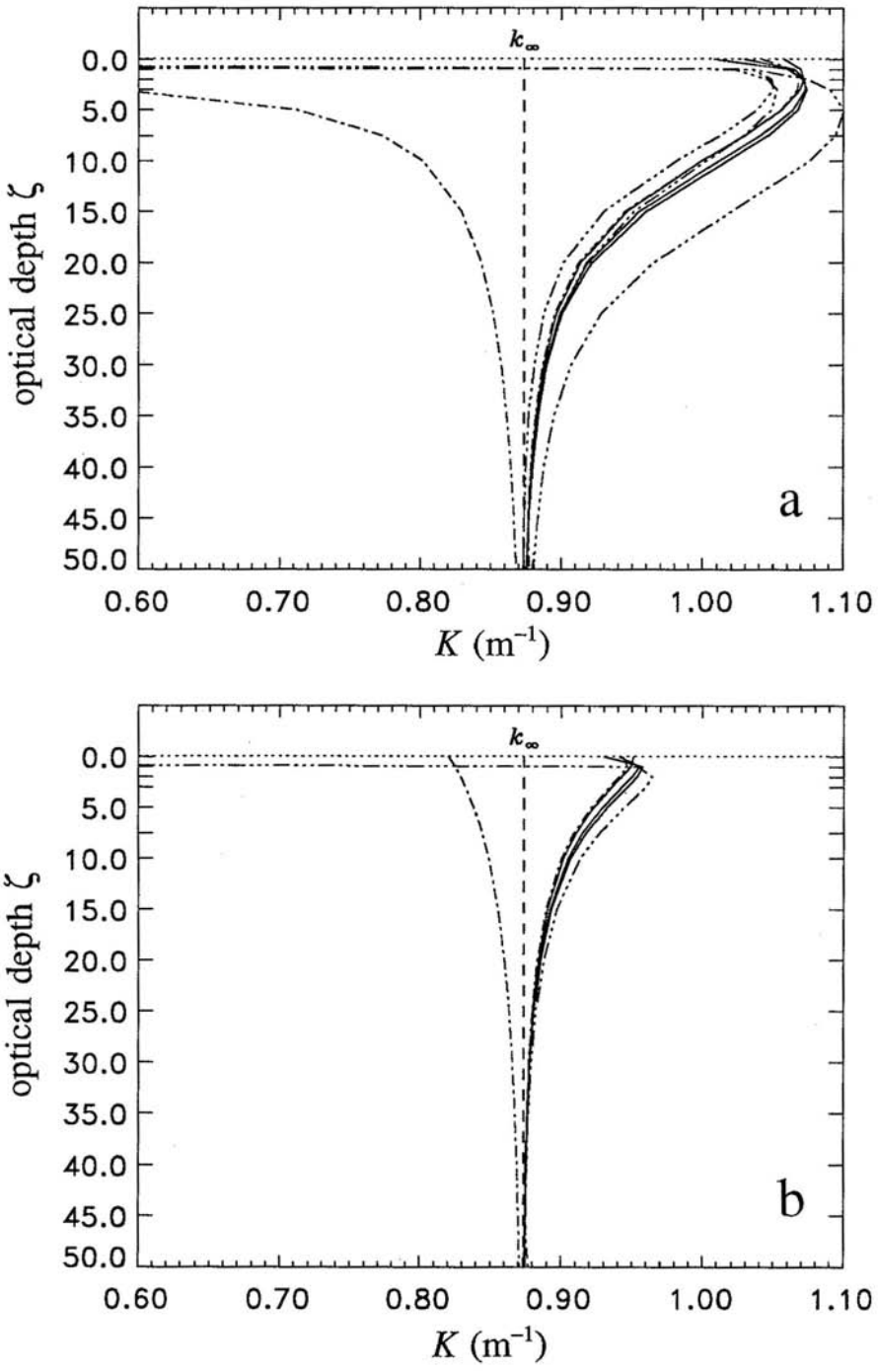

Fig. 9.6. Depth dependence of selected K-functions in highly absorbing water ($\omega_o = 0.2$); otherwise the parameters are the same as for Fig. 9.5.

Mathematically, the rate of approach to L_∞ is governed both by the remaining eigenvalues $\kappa_2, \kappa_3, ..., \kappa_q$ and by the initial conditions $\underline{a}^{\pm}(w)$, as seen in Eq. (9.79). If κ_2 is close to $\kappa_1 = \kappa_\infty$, and if the corresponding eigenvector is strongly "excited" by the incident radiance [i.e., if the eigenvector has a large initial value $a_2^{\pm}(w)$], then the approach to the asymptotic value will be slow. These matters are discussed in some detail in McCormick (1992a).

An integral equation for the asymptotic radiance

If we return to the RTE for homogeneous, source-free water, Eq. (9.7), and assume that the radiance has the form seen in Eq. (9.84), we immediately obtain

$$(1 - \kappa_\infty \mu)\, L_\infty(\mu) \;=\; \omega_o \iint_{\Xi'} L_\infty(\mu')\, \tilde{\beta}\,(\mu',\phi' \rightarrow \mu,\phi)\, d\mu'\, d\phi' \,. \qquad (9.87)$$

This equation is an *integral equation for the shape* $L_\infty(\mu)$ *and decay rate* κ_∞ *of the asymptotic radiance distribution*. Given the IOP's ω_o and $\tilde{\beta}$, we can solve Eq. (9.87) for the corresponding $L_\infty(\mu)$ and κ_∞. Another form of Eq. (9.87), often seen in the literature, is

$$(1 - \kappa_\infty \mu)\, L_\infty(\mu) \;=\; 2\pi\omega_o \int_{-1}^{1} L_\infty(\mu')\, h(\mu',\mu)\, d\mu' \,,$$

where the *redistribution function* $h(\mu',\mu)$ is the azimuthally averaged phase function (van de Hulst, 1980)

$$h(\mu',\mu) \;\equiv\; \frac{1}{2\pi} \int_0^{2\pi} \tilde{\beta}\,(\mu',\phi' \rightarrow \mu,\phi)\, d\phi' \,.$$

For the case of isotropic scattering, $\tilde{\beta} = 1/4\pi$, the solution of Eq. (9.87) has the simple form

$$L_\infty(\mu) \;=\; \frac{1 - \kappa_\infty}{1 - \kappa_\infty \mu} \,, \qquad (9.88),$$

where we have normalized $L_\infty(\mu)$ to 1 at $\mu = 1$ (or $\theta = 0$, the nadir direction); recall Eq. (5.34). Note that this $L_\infty(\mu)$ has the shape of an ellipse whose major axis is oriented vertically. The corresponding value of κ_∞ is the solution of the transcendental equation

$$1 = \frac{\omega_o}{2\kappa_\infty} \ln\left(\frac{1+\kappa_\infty}{1-\kappa_\infty}\right),$$

as can be seen by substitution of Eq. (9.88) into Eq. (9.87).

Kattawar and Plass (1976) obtained an analytic solution of Eq. (9.87) for the Rayleigh phase function $\tilde{\beta}(\psi) = (3/16\pi)(1 + \cos^2\psi)$. However, for other phase functions, in particular for those like $\tilde{\beta}_p$ of Table 3.10, the solution of Eq. (9.87) must be obtained numerically. Solving the integral Eq. (9.87) is mathematically equivalent to solving the eigenmatrix equation as described above.

Equation (9.87) has been used in several studies of asymptotic light fields; see in particular Prieur and Morel (1971) and Kattawar and Plass (1976).

9.7 Problems

9.1 Expand the Rayleigh phase function

$$\tilde{\beta}(\psi) = \frac{3}{16\pi}\left(1 + \cos^2\psi\right)$$

in a series of Legendre polynomials.

9.2 Verify the orthogonality relation (9.3) by explicit calculation using P_3 and P_4.

9.3 Substitute the Delta-*M* approximation (9.22) into the RTE (9.7) and show that the resulting equation involving $\tilde{\beta}^*$ has the same *form* as Eq. (9.7), if the optical depth and the albedo of single scattering are redefined as

$$\zeta^* \equiv (1 - 2\omega_o f)\,\zeta$$

and

$$\omega_o^* \equiv \left(\frac{1-f}{1-2\omega_o f}\right)\omega_o,$$

respectively.

9.4 Suppose that the optical depths ζ and w are very close together, i.e. $\zeta - w << 1$. Then the exponential in Eq. (9.54) can be approximated by

$$e^{\underline{\kappa}(\zeta - w)} \approx \underline{I}_{2q} + \underline{\kappa}(\zeta - w) .$$

Use this approximation along with Eq. (9.71) and the matrix equivalent of Eq. (7.51) to show that, to first order in $\zeta - w$,

$$\underline{T}(\zeta,w) \approx \underline{I}_q - \hat{\underline{\tau}}(\zeta - w)$$
$$\underline{R}(\zeta,w) \approx \hat{\underline{\rho}}(\zeta - w) .$$

These relations highlight the physical interpretations of $\hat{\underline{\tau}}$ and $\hat{\underline{\rho}}$ as representing (in spectral form) the transmittance and reflectance of thin slabs of water.

9.5 Partition a homogeneous, source-free water body into the surface plus the water: $S[a,b] = S[a,w] \cup S[w,b]$. Then formulate appropriate global interaction principles for depths (a,w,b), and use the associated union and imbed rules, as in Chapter 7, to derive Eq. (9.77). How does this result compare with that obtained in problem 4.5?

9.6 Qualitatively explain the shapes of the asymptotic values of the AOP's seen in Fig. 9.4 in terms of the shapes of the phase functions and the values of ω_o.

9.7 Consider Fig. 9.5, which shows K-functions in terms of optical depth ζ for $\omega_o = 0.8$. To what geometric depth z does $\zeta = 50$ correspond, if the turbid water has $a = 0.4$ m^{-1} and $b = 1.6$ m^{-1}? What is the dimensional k_∞ value? Repeat this problem for the clear-water case of Fig. 9.6, assuming that $a = 0.04$ m^{-1} and $b = 0.01$ m^{-1}.

9.8 Suppose that we have isotropic scattering, $\tilde{\beta} = 1/4\pi$, and $\omega_o = 0.7$. Show by explicit calculation using Eq. (9.86) that the corresponding asymptotic radiance distribution has the form

$$L_\infty(\mu) = \frac{1 - \kappa_\infty}{1 - \kappa_\infty \mu} ,$$

where $\kappa_\infty \approx 0.8286$.

9.9 Develop an eigenmatrix theory for *irradiances* in source-free, homogeneous water. Start with the source-free, depth-independent version of Eq. (7.37),

$$\frac{d}{dz}\underline{E}(z) = \underline{E}(z)\,\underline{K} ,$$

where now $\underline{K}$ is a 2×2 matrix of the form

$$\underline{K} = \begin{bmatrix} -\tau_{uu} & \rho_{ud} \\ -\rho_{du} & \tau_{dd} \end{bmatrix}.$$

The τ's and ρ's are now numbers with dimensions of m^{-1}, which are assumed known.

Parallel the developments in Sections 9.2-9.6, noting where the results developed at the radiance level also hold for irradiances and *where they do not*, because $\underline{K}$ is no longer anti-symmetric ($\rho_{ud} \neq \rho_{du}$), or because $\tau_{uu} \neq \tau_{dd}$. By explicit calculation, find the two eigenvectors $\underline{e}^{\pm}$ and dimensional eigenvalues $k^{\pm}$ of $\underline{K}$ in terms of the τ's and ρ's. Do $k^{\pm}$ still have the form $k^{\pm} = \pm k$? Express $R(\infty)$ and the asymptotic decay rate $k_{\infty} = -k^{-}$ in terms of the τ's and ρ's.

When you are done developing your theory, you can check it against the following "observations" (which were numerically generated for a natural water body at green wavelengths):

$$\underline{K} = \begin{bmatrix} +1.0264 & 0.1810 \\ -0.0225 & -0.4065 \end{bmatrix} \qquad (m^{-1}),$$

$$k^{+} = 1.0236\ m^{-1} \qquad k^{-} = -0.4036\ m^{-1}$$

$$R(\infty) = 0.0157 \qquad k_{\infty} = 0.4036\ m^{-1}$$

$$\underline{e}^{+} = C\begin{bmatrix} 0.1810 \\ -0.00285 \end{bmatrix}, \qquad \underline{e}^{-} = C\begin{bmatrix} -0.00285 \\ 0.0225 \end{bmatrix},$$

where C is an arbitrary constant.

Next Chapter >>